Hydrogeology and assessment of the effect of oil-production activities in the Midway Valley area, western Kern County, California

Janice M. Gillespie[1]*, Riley S. Gannon[1], Lyndsay Ball[2], John G. Warden[1], Rhett R. Everett[1], Michael Stephens[3]

[1] U.S. Geological Survey, California Water Science Center, San Diego, CA 92101

[2] U.S. Geological Survey, Geology Geophysics and Geochemistry Water Science Center, Lakewood, CO 80225

[3] U.S. Geological Survey, California Water Science Center, Sacramento, CA 95819

*Corresponding author: jmgillespie@usgs.gov

Hydrogeology and assessment of the effect of oil-production activities in the Midway Valley area, western Kern County, California

Janice M. Gillespie[1]*, Riley S. Gannon[1], Lyndsay Ball[2], John G. Warden[1], Rhett R. Everett[1], Michael Stephens[3]

Abstract

The southwestern San Joaquin Valley, California includes oil fields and oil-field water disposal facilities, (ponds and injection wells). The Tulare Formation and overlying alluvium comprise the main aquifers in the study area and are commonly used for produced water disposal. Water quality in the aquifers is naturally brackish (total dissolved solids (TDS) 3,000-10,000 mg/L) across most of the area.

Geophysical logs are useful in determining salinity variations within aquifers including the depth at which TDS>10,000 mg/L, often used as a criterion for evaluating underground injection permits. The depth to water with 10,000 mg/L TDS ranges from 366 m in the northwest to ~ 1,500 m in the southeast. Water table elevations from porosity logs and groundwater wells indicate the water table slopes south-southeast, showing predominant groundwater flow direction from oil field disposal areas toward better quality groundwater east of the oil fields. However, groundwater velocities <60 meter/year indicate it could take over a century to affect fresher groundwater to the east.

Electric log data show formation resistivity near some disposal facilities has decreased over time, indicating that the salinity of the brackish aquifer has increased due to disposal of saline produced water. Evidence of increased salinity over time in water saturated sand intervals >1.5 km from disposal facilities may be caused by mechanical failures and/or incomplete borehole seals in poorly constructed or abandoned wellbores prevalent throughout the study area.

[1] U.S. Geological Survey, California Water Science Center, San Diego, CA 92101
[2] U.S. Geological Survey, Geology Geophysics and Geochemistry Water Science Center, Lakewood, CO 80225
[3] U.S. Geological Survey, California Water Science Center, Sacramento, CA 95819

*Corresponding author: jmgillespie@usgs.gov

Introduction

The effects of oil and gas production on groundwater quality is of increased concern in many areas of the US. The implications are especially important in areas that use large amounts of groundwater for irrigated agriculture and domestic use. The study area of this paper lies in western Kern County, California—an area with vast, but declining, oil reserves (Fig 1). In 2019, Kern County was ranked the #7 oil-producing county in the US [1] --down from #3 in 2013 [2]. It produces 71% of California's total oil and 3% of total oil in the US [1]. Western Kern County is also an important agricultural producer. Kern County was named the #1 agricultural producing county in the nation in 2021, narrowly edging out nearby Fresno and Tulare counties [3]. Agriculture in Kern County uses approximately 2.3 million acre-ft (MAF) of water per year—approximately 36% of this water is groundwater [4]. Western Kern County lies within the southern San Joaquin Valley (SJV) in the Tulare Lake hydrologic region. This region uses more water than any other region in California and 69% of the region's water use is met by groundwater (> 8 MAF). It is considered a critically overdrafted groundwater basin [5].

Fig 1. Satellite photo of the study area showing oil fields and important geographic and geologic features.

The location of the photo is shown in the red box in the inset map of California. Basemap from Earthstar Geographics | CalGEM GIS Unit | Geologic Energy Management Division, California Department of Conservation. | City of Bakersfield, California State Parks, Esri, TomTom,

Garmin, SafeGraph, METI/NASA, USGS, Bureau of Land Management, EPA, NPS, USDA, USFWS.

Because groundwater is so important to the national and state economies, the California State Water Resources Control Board (Water Board) implemented a program to monitor water quality in oil and gas producing area beginning in 2015. Known as the Oil and Gas Regional Monitoring Program (RMP), these investigations focus primarily on areas with groundwater near well stimulation (hydraulic fracturing), enhanced recovery (steam and water flooding), produced water disposal by surface sumps or underground injection, and/or naturally occurring shallow oil and gas deposits.

The focus of this study is the Midway Valley, an area of long-term, intensive oil and gas development that drains hydrologically into the San Joaquin Valley and associated Central Valley aquifer system [6]. An analysis of regional shallow groundwater quality in the same study area [7] found effects of legacy surface disposal of oil field water in some groundwater areas east of the oil fields where produced water was routed down surface drainages before about 1960 into the San Joaquin Valley, bringing produced water closer to groundwater. However, that study only looked at groundwater in the upper few hundred feet of the aquifer system east of the oil fields, lacked information at greater depths due to the absence of deeper wells, and had little groundwater sample data within the oil fields. This study, by using analysis of oil well borehole geophysical logs, helps fill in information on the thickness of fresh (TDS <3,000 mg/L) and brackish (TDS 3,000-10,000 mg/L) groundwater at greater depths and provides a much greater density of data within the oil fields.

Study Area

The current study focuses on the Midway Valley area located within the southwestern part of the San Joaquin Valley. This area lies within the westernmost part of the Maricopa-Tejon subbasin in the southernmost part of the San Joaquin Valley (Fig 1) in western Kern County, California. The Maricopa-

Tejon subbasin is separated from the larger northern portion of the SJV by the Elk Hills anticline and the Bakersfield Arch and is bounded to the south by the San Emigdio and Tehachapi ranges which form the southern margin of the SJV. Folded sedimentary rocks of the Temblor Range bound the area on the west and felsic to intermediate igneous rocks of the Sierra Nevada on the east. Bartow (1991) [8] notes that this sub-basin probably has the most complex tectonic history and contains the thickest Cenozoic deposits in the SJV. The southernmost part of the sub-basin, which contains the thickest deposits, is locally known as the Maricopa depocenter [9].

At the end of the Mesozoic, the San Joaquin Valley was a forearc basin lying between the Pacific-North American convergent margin subduction zone to the west and the associated magmatic arc of the Sierra Nevada to the east [8]. The intersection of the east Pacific Rise spreading center with the subduction zone occurred during Cenozoic time [10] creating a transform margin exemplified by the right-lateral San Andreas transform fault. Evidence of southwest-northeast compression in the area is evident during Cenozoic time [8]. Folding and thrust faulting are driven by transpressional forces along the San Andreas transform fault which lies approximately 8 km (5 mi) west of the study area. The Midway Valley lies within the fold-thrust belt and occupies a SE-plunging syncline between the Midway Sunset and Buena Vista anticlines in the southwestern SJV, California (Fig 2).

Fig 2. Elevation of the base of the Tulare Formation/base Tulare lithosome

Where the contact between the Tulare and underlying San Joaquin formations is indistinguishable, the mapped horizon is the base of the Tulare lithesome (contours in feet). Wells shown are those used to construct the map and detailed information is available in the associated data release [11]. The stars show the locations of the well logs in figure 3.

The two largest oilfields in the study area are the Midway-Sunset and Buena Vista Oil Fields (Fig 1). As of 2021 (the most recent publicly available report from CalGEM (California Geologic Energy Management),

Midway Sunset was the largest oil-producing field in California [12]. The first production from the field occurred about 1890 [13]. Most of the oil produced from the field is heavy to intermediate (10 to 28 degrees API). The heavier crudes are produced by steamflood and cyclic steaming. Buena Vista Oil Field was discovered in 1909 and produces medium to light crude oil (18 to 36 degrees API) as well as dry gas [13]. Both fields produce large amounts of water along with the oil and, because the water is too saline for most uses, it is usually disposed of by infiltration in ponds or injection into shallow aquifers. Davis et al. (2024) [14] notes that the total produced water volume disposed in ponds is approximately 1.6 m^3 (9.8 Bbbls) alone. Additional produced water is injected into water disposal wells in the Tulare Formation and overlying alluvium as well as some of the deeper Pliocene and Miocene sands [15]. This manuscript describes analysis of the aquifers in the Midway Valley study area to determine their vertical and lateral extent, groundwater quality and effects of water disposal practices on groundwater quality.

Stratigraphy

While the northern part of the SJV was the site of primarily nonmarine deposition throughout the late Cenozoic, the southern SJV contains sedimentary rocks deposited in both non marine and marine environments representing a wide range of depths. The late Cenozoic stratigraphic history of the southern SJV is generally characterized as changing from deep marine conditions during late Miocene time to shallow marine deposits in Pliocene time and, finally, to fluvial and lacustrine deposits in the Pleistocene. A stratigraphic column of the southern San Joaquin Valley is provided in Figure 3.

Fig 3. Stratigraphic column for the San Joaquin Valley.

The formations outlined in red are discussed in this paper. The electric logs shown to the left of the stratigraphic column highlight the differences in thickness and lithology of the Tulare aquifer and overlying alluvium in both the western and eastern parts of the study area. Green highlighted intervals in center of well 02984446 log indicate oil shows. The locations of these

wells are shown on the map in figure 2. Resistivity > 3 ohm-m highlighted in yellow. Stratigraphic column modified from Scheirer and Magoon (2007) [16].

Late Miocene

Late Miocene deposition in the study area is represented by the deep marine Reef Ridge Shale and Monterey Formation which contain sedimentary rocks deposited in deep sea pelagic and turbidite environments. The turbidite sandstones form important reservoirs in the Midway Sunset and Buena Vista Oil Fields.

Pelagic environments in the upper Monterey Formation are characterized by siliceous shales, cherts and diatomite deposits. The western SJV was the site of large diatomite blooms as a result of cooling climatic conditions and upwelling currents along the western North American margin [17]. As these siliceous algae died, they sank and accumulated on the seafloor. The diatomite produces oil within parts of the study area. Due to the generally low permeability and high porosity of diatomite, the oil is produced using fracturing and, sometimes, steaming techniques [18].

Pliocene

As sediments from the erosion of the surrounding mountain ranges began to fill the southern SJV, deep marine deposition was replaced by shallow marine deposits during Pliocene time [19]. These deposits are represented by the Etchegoin and overlying San Joaquin Formations. In the western part of the study area, the contacts between the Monterey, Etchegoin and San Joaquin Formations are represented by angular unconformities and the Etchegoin and San Joaquin Formations are absent in the westernmost part of the Midway-Sunset Oil Field. The thickness of the strata removed by erosion along the unconformities decreases eastward into the deeper portion of the Maricopa sub-basin and the sedimentary section thickens. In the study area, the geology of the San Joaquin Formation changes from

a relatively thin section of mostly clay containing isolated marine sands in the west to a thick series of overlapping sands that are difficult to distinguish from the overlying nonmarine Tulare Formation in the east and south. The Etchegoin Formation and the Top Oil sand in the lower part of the San Joaquin Formation are important oil reservoirs in the eastern part of the Midway Sunset Oil Field and in the Buena Vista Hills Oil Field. They are also used for produced water disposal.

Pleistocene and Recent

Pleistocene and Recent deposition is represented by the Tulare Formation and overlying alluvium. The Tulare Formation is unconsolidated and was deposited in a series of fluvial channels, alluvial fans, lakes and floodplains as the sea retreated from the SJV [20]. The lacustrine Amnicola clay where present divides the upper Tulare Formation from the lower. The upper part of the Tulare Formation contains thick sands whereas sands in the lower part are much thinner and more numerous. In the west, the contact between the Tulare and underlying Etchegoin and San Joaquin Formations is an angular unconformity and, in the westernmost part of the Midway-Sunset Oil Field, the Pliocene formations are removed by erosion and the Tulare lies unconformably upon folded sediments of the Monterey Formation before pinching out along the foothills of the Temblor Range [13]. Most of the oil produced from the Tulare Formation comes from the lower part of the formation [9]. The Tulare Formation is also used for produced water disposal by injection wells and, where the overlying alluvium is absent, infiltration of produced water from surface ponds can reach the Tulare Formation.

The Tulare Formation is unconformably overlain by alluvium throughout most of the Midway Valley. The alluvium is absent over the crests of the anticlines and thickens into the syncline of the Midway Valley and the Buena Vista lakebed to the south and east. The alluvium appears to be over 914 m (3000 feet) thick in the Maricopa depocenter (Fig 4); however well control within the upper 305 m (1000 feet) of the section is poor in this area making correlations difficult. Cores from the alluvium and upper

Tulare Formation in the USGS MSBV well indicate that the alluvium contains higher percentages of clay and detrital diatomite than the underlying Tulare Formation [21]. This mineralogical composition results in higher porosity and higher specific retention values [21] in the alluvium.

Fig 4. Thickness and extent of the alluvium in the study area.

The erosional edge of the alluvium is approximately rendered as defined by Dibblee and Minch (2005 a, b and c) [22-24], WZI (1988) [25] and this study. The alluvium is absent in the western part of the Midway Sunset oilfield and over the east and west domes of the Buena Vista oil field. It reaches a thickness of approximately 910 m (3000 feet) in the western part of the Maricopa depocenter in the southeastern part of the study area.

At the base of the alluvium is a clay known locally as the basal alluvial clay that may be up to 150 m (500 ft) thick [25] and, where it is present, separates the alluvium and Tulare Formation into separate aquifers. The total thickness of the Tulare Formation and overlying alluvium is shown in Figure 5.

Fig 5. Depth to the base of the Tulare Formation/Tulare lithosome in the study area.

This map is an approximate measure of the thickness of the combined alluvium/Tulare aquifer (contours in feet). However, the lower part of the aquifer system (within the interval below the Amnicola clay) contains water with > 10,000 mg/L TDS.

The alluvium is not known to produce oil in the study area, but it is sometimes used for produced water disposal via both injection and infiltration from surface impoundments. Depth values for the base of the alluvium, base of the Amnicola Clay and base of Tulare Formation used in this study are available in the accompanying data release [11].

Methods

Mapping

In many actively subsiding basins such as the San Joaquin Valley, formations are poorly exposed at the surface or not exposed at all. In the Midway Valley study area, the San Joaquin and Etchegoin Formations do not outcrop at land surface—even along the basin margins—because they have been removed along an angular unconformity between the Tulare and Monterey Formations. In addition, the sedimentary facies of the formations may be different in the basin depocenter than they are along the basin margins. For example, finer-grained lacustrine and lacustrine delta facies may be more common along the basin axis while coarser-grained alluvial fan deposits may be more prevalent along the basin margins. Geophysical logs in wells drilled in the basin can help document these changes in depositional style to see how the thickness and composition of the formations change relative to their location within the basin setting and to distinguish formation contacts and vertical changes in depositional facies over time.

The major aquifers in the area are the Tulare Formation and overlying alluvium. Geophysical log data were used to pick formation boundaries between the alluvium and the Tulare Formation (Figs 3, 4), between the upper and lower Tulare Formation (where the Amnicola clay is present as a confining layer), and between the Tulare and underlying marine San Joaquin and Etchegoin Formations (Figs 3, 5) [11].

The contact between the Tulare Formation and the overlying alluvium is unconformable in the western part of the study area but may be conformable farther east. Sand layers in the Tulare Formation are also thicker and more well-defined than those in the overlying alluvium. The alluvial deposits typically have higher porosity on density-neutron logs (Fig 6)—possibly reflecting the greater percentage of detrital diatomite in the alluvium observed in cores from the USGS MSBV monitoring well [21] (diatomite can have porosities as high as 70%). The change in porosity from the Tulare to the

alluvium is very abrupt in the western part of the study area (Fig 6a) where the contact is unconformable but more gradational in the east (Fig 6b) where the contact is more conformable. The greater separation between the density and neutron porosity values in the alluvium also indicates a greater clay content in the alluvium. The contact between the Tulare and alluvium is also characterized by lower gamma ray log values in the Tulare Formation and a shift to more negative SP log values in the Tulare Formation. This may be due to higher overall clay content in the alluvium than in the Tulare Formation as observed in the USGS MSBV cores [21].

Fig 6. Density and neutron log porosity values for the alluvium and Tulare Formation.

Density (blue) and neutron (red) porosity log values for the alluvium and Tulare Formation in a) the USGS MSBV monitoring well in the Midway Valley syncline which represents the western part of the study area where the contact between the alluvium and Tulare Formation is represented by an unconformity and b) the D-1 monitoring well in the Buena Vista lakebed representing the eastern part of the study area where the stratigraphic section is thicker and the contact is more conformable. The contact is sharp and unconformable in the west (Fig 6a) and becomes more gradational and more difficult to ascertain in the east (Fig 6b). Only data from water saturated intervals were used in the plots.

The Tulare Formation is divided into upper and lower portions where a pronounced clay layer—the Amnicola clay—is present. This clay layer is well-developed in the western and central parts of the study area where it has not been removed by erosion.

The Tulare Formation typically contains a higher percentage of sand than the underlying Pliocene formations in the western part of the study area. Because the Tulare sands are fluvial rather than marine, their discontinuous and overlapping character on the resistivity and spontaneous potential (SP) logs makes them more difficult to correlate between wells than sands in the marine sections of the San Joaquin and Etchegoin Formations which are separated by thick clay intervals. In the eastern part of the

study area, the Tulare Formation lies conformably upon the San Joaquin Formation. Here, both contain a thick series of overlapping sands characteristic of fluvial environments and the contact between the formations is difficult to pick on electrical logs. In these areas, the thick sequence of fluvial sands is mapped herein as a single lithosome--the Tulare lithosome-- that contains both the Tulare Formation and the upper, fluvial part of the San Joaquin Formation (Figs 3, 5).

Hydrogeology

Density-neutron log and, in some cases, resistivity logs were used to map the base of the vadose zone, or water table, within the oil fields in the study area. The density log measures porosity by determining the bulk density of the interval. The neutron porosity log measures porosity by measuring the amount of hydrogen atoms within an interval. Because water, oil and clay layers contain more hydrogen atoms than gas or air, the neutron log measures greater porosity in liquid-saturated intervals and reads higher porosity in clays than the density log due to the presence of OH^- groups in the clay lattice. The vadose zone and gas-filled sands contain fewer hydrogen atoms than liquids and, consequently, the neutron log sees these intervals as abnormally low porosity zones. If the sand is filled with air or gas, the bulk density is much lower than a water or oil filled sand so the density log records abnormally high porosity in the unsaturated zone. Therefore, the normal behavior of the two curves is reversed relative to each other in the vadose zone with the density curve reading higher porosity than the neutron—a phenomenon known as cross over. Sands below the interval of cross-over lie below the water table so the depth to the water table lies at the base of the sands exhibiting cross-over on the log (Fig 7a) and these values were used to construct the map in Figure 7b. Wells used to construct the map in Figure 7b are available in the associated data release [11].

Fig 7. **Well log showing density-neutron log cross over used to map the water table elevation**.

a) An example of the USGS MSBV well log showing density-neutron log cross over (shaded yellow) used to map the elevation of the water table. Pink rectangles on MSBV log denote salinity intervals higher than native groundwater. b) Map of the elevation of the base of the vadose zone (water table) created from density neutron log cross-over. Wells shown are those used to create the map and the data are available in the associated data release. Because depth values are only available for the date the well was logged, this map represents water table elevations for a multitude of dates spanning several decades. In most cases, the water table lies within the Tulare Formation. Areas circled in red on map indicate saline groundwater perched in the alluvium resulting from produced water disposal practices. Major produced water disposal sumps are shown in light blue [14]. The locations highlighted in magenta indicate wells in which the water table lies within the alluvium or there are multiple water tables—one in the alluvium and one in the Tulare Formation as shown by the two intervals of yellow-shaded density-neutron log cross-over in the USGS MSBV log in 7a (location shown by star on map). Cross section A-A' is shown in Fig 9.

Density-neutron measurements correspond to the time at which the well was drilled and logged, therefore the map in figure 7b represents water table elevations for a variety of dates spanning several decades. The focus of this analysis is on water table elevations within the oil fields where water level data were previously sparse. In contrast, oil well geophysical log data are sparse east of the oil fields.

Many of the wells in the area were drilled prior to the development of density-neutron logs in the 1970's. In these older wells, resistivity values can provide an approximation of the depth to the water table at the time the well was drilled because groundwater salinity in the area generally exceeds 3000 mg/L TDS even at depths above 305 m (1000 ft). Therefore, the saturated sands below the water table have a markedly lower resistivity than the air-filled sands above and, in these cases, resistivity logs can be used to determine the depth to the water table, albeit with less certainty than wells with density-

neutron logs. The resistivity method cannot be used in areas where shallow oil is present near the water table because hydrocarbons have high resistivity and their response on the resistivity logs is similar to that of air-filled sands. If there is no evidence of hydrocarbon shows or production near the water table in nearby well histories, these older wells were also used to generate the map in Figure 7b [11].

Many definitions of fresh, brackish, and saline groundwater have been used in the literature (Stanton et al. 2017). In this manuscript we use definitions of fresh (<3,000 mg/L), brackish (3,000-10,000 mg/L), and saline (>10,000 mg/L), used in other groundwater studies in the western San Joaquin Valley where naturally occurring groundwater with TDS>1,000 mg/L is widespread [26, 27, 7]. Salinity refers to the concentration of salts in the water, including major inorganic ions like sodium, calcium, chloride, bicarbonate, and sulfate. TDS includes these salts and other dissolved substances such as minor ions and organic compounds. However, in the study area, with widespread brackish water and high concentrations of inorganic salts, salinity and TDS are synonymous and both terms are used in this manuscript.

Geophysical logs can be useful in determining salinity variations within aquifers including determining the depth of TDS thresholds at 10,000 milligrams per liter (mg/L) (one of the criteria for delineating Underground Sources of Drinking Water or USDW) and, with less precision, the Base of Fresh Water (BFW), which is approximately 2,000 to 3,000 mg/L [28-30]. These salinity thresholds have been considered, along with other criteria, in regulatory permitting decisions for underground disposal of waste fluids [30, 31]. The Tulare Formation is exempt (that is not serving as a source of drinking water and allowed to be used for oil extraction and water disposal) in the Buena Vista Oil Field and in parts of the Midway-Sunset Oil field [32]. However, the eastern part of the study area lies outside these exemption areas, so it is useful to understand how salinity gradients (TDS vs. depth) vary across the area. The alluvium is not exempt.

In sands containing little clay and no hydrocarbons, Archie's [33] equation can be modified to approximate groundwater resistivity (R_w) values using geophysical logs that measure bulk resistivity of a water-filled material obtained from the deep resistivity curve on the electric log and porosity obtained, in this case, from the density-neutron log as well as temperature (Equation 1).

$$R_w = Ro * (\phi^m / a) \quad \text{Equation 1}$$

Where Ro = bulk resistivity from the deep resistivity log and ϕ = average porosity from the density-neutron logs. The Archie exponents '*a*' and '*m*' where *m* (unitless) is the cementation factor and *a* (also unitless) is the tortuosity factor can be obtained by special core analysis but these types of analyses are rare and many studies use published values for sediments deposited in similar environments and with similar degrees of cementation such as those by Winsauer et al. [34] or Carothers [35]. Fortunately, core analyses to determine the formation factor were performed on five intervals in the Tulare Formation from a water disposal well in the Buena Vista field (API 0402959052) and are available in the CalGEM online DATA file [36]. The value for *a* was held constant at 1 and the formation factor derived from core analysis was solved for *m*. The calculated values for *m* ranged from 1.61 to 1.87 with a mean value of 1.79 (standard deviation of 0.1) and a median value of 1.8. Therefore, our salinity calculations use *a* = 1 and *m* = 1.8 based on the core analysis results.

Porosity values were averaged for the density and neutron log to derive a porosity value at each depth for which salinity was calculated. The density value was weighted twice as much as the neutron value because the neutron value is influenced by the presence of OH^- groups on clays and, therefore tends to overestimate porosity (Archie's equation is designed to work best in sands with a low clay content). To determine clay volume, the largest separation between the density and neutron curves over the interval analyzed on the log was noted and assumed to represent 100% clay content. The ratio of density-neutron curve separation in the intervals used for salinity calculations was divided by the 100% clay value and, if the ratio exceeded 0.25, the interval was not used to calculate salinity.

By correcting for the effects of temperature, the resistivity can be converted to salinity values using equations or empirical charts assuming that the dominant ions in the water are Na and Cl. Here Archie's equation is used to calculate water resistivity and the Bateman and Konen [37] equations (2) and (3) incorporate R_w and temperature (in degrees F) at the desired depth to provide values for salinity as NaCl.

$$\text{TDS mg/L NaCl @ } 75^{o}\text{F} = 10^{((\log Rw75 - 0.0123)/0.955)} \qquad \text{Equation 2}$$

$$R_{w75} = R_w \times (T + 6.77)/81.77 \qquad \text{Equation 3}$$

Wells used for calculations are those that were logged with induction resistivity and density-neutron logs and had relatively few borehole irregularities such as borehole washouts in the caliper log. Intervals containing air, oil, gas, and clay volumes > 25% (as calculated from the density-neutron) were avoided. The depth at which the calculated salinity reached 10,000 mg/L was noted for wells that met these criteria. The calculations from these logs are provided in the data release [11].

Calculated values for salinity are similar to lab analyses of groundwater samples from three monitoring wells at the USGS MSBV site (32S24E21G01) drilled in the Midway Valley in 2023 (Fig 7a) [21] with the exception of the high salinity zone in the overlying alluvium where the calculated value was about 5000 mg/L lower than the measured salinity of 24,600 mg/L but still indicates perched high-salinity groundwater. With few exceptions, the salinity of the native groundwater in the study area is generally greater than 3,000 mg/L so our calculations focused on the depth at which the salinity reached 10,000 mg/L.

Only about 45 wells in the area met the criteria described above for use in the Archie calculations and could be used to generate a map showing the depth to 10,000 mg/L TDS. Most wells in the area were drilled prior to the advent of density-neutron logs in the 1970's and have only electrical logs (resistivity and SP). In order to construct a map of depth to 10,000 mg/L with greater well control, Archie-

calculated salinity vs. bulk resistivity plots were created for 39 wells within the study area (Fig 8). Average values for bulk resistivity (R_o) were determined in intervals with calculated salinity of 9500 to 10,500 mg/L, approximating the 10,000 mg/L threshold. The average bulk resistivity value for 10,000 mg/L is 3 ohm-m (+/- 0.8, n = 67). This allowed us to construct a map showing the depth to 10,000 mg/L based on a deep resistivity of 3 ohm-m that includes data from 560 wells with induction resistivity logs in the study area [11]. However, without measured values for porosity, the estimated depths to 10,000 mg/L are more uncertain than if porosity values were used to constrain the TDS calculations.

Fig 8. Calculated salinity vs. resistivity plot from 39 wells in the study area.

This plot was used to determine the approximate resistivity at which groundwater salinity exceeds 3000 mg/L (brackish) and 10,000 mg/L (saline). Fifty-nine values of calculated salinity between 2,500 and 3,500 mg/L (BFW) indicate that the average resistivity is approximately 12.2 ohm-m (+/- 3.5 ohm-m). Sixty-seven calculated salinity values between 9,500 and 10,500 mg/L (USDW) indicate the average resistivity is approximately 3 ohm-m (+/- 0.8 ohm-m). The green vertical line shows the average value of resistivity for 9500-10,000 mg/L TDS and the associated box shows the standard deviation of the values. The blue vertical line and associated box shows the average resistivity value and standard deviation for 2,500-3,500 mg/L. The average porosity values for 2,500-3,500 mg/L is 0.32 (+/- 0.04) and for 9,500-10,500 mg/L is 0.33 (+/- 0.04).

Well Mechanical Integrity

Oil well histories from 2400 wells in the study area were also examined for mechanical and construction issues that have the potential to provide vertical pathways for vertical fluid movement. Issues noted included casing holes, collapsed casing, crooked casing and plugged and abandoned wells with incomplete seals in well casing and/or annular borehole space. The well histories examined for this

study comprise slightly less than 1% of the 33,700 wells in the study area. These wells included wells used for correlation throughout the study area and wells within the Midway Valley syncline. The date the well was logged or the earliest date of water shut off tests (for wells without logs) were noted as well as the date the mechanical issue was first noted in the well history. Mechanical issues in the liners covering the producing zones were not noted as the liners are often isolated from the overlying groundwater sands by cement. Where liners are not present and oil is produced from perforated casing, the issues were noted even though these zones are also often isolated by cement. Producing well blowouts and surface expressions are also noted because these may reflect poor cement bonding and result in migration of fluids behind pipe. The data are available from [11].

Results

Mapping

Mapping results indicate that the alluvium is thickest, over 914 m (3000 feet), in the southeastern part of the study area (Fig 4). The combined alluvium/Tulare lithosome is also thickest in this area, over 2438 m (8000 ft) thick (Fig 5), indicating that the Tulare lithosome is about 1524 m (5000 feet) thick. The thickness of the alluvium/Tulare lithosome decreases to the west.

Water table elevations estimated from porosity logs within the oil fields indicate the predominant groundwater flow direction is east to northeast from oil field disposal areas toward better quality groundwater east of the oil fields (Fig 7b). Groundwater levels measured in water wells are available east of the oil fields in the study area and also generally indicate groundwater table elevations sloping to the east-northeast away from the oil fields [38]. However, groundwater velocities calculated from known plumes from monitored surface disposal areas in the oil fields are <60

m/year (197 ft/yr) [7], indicating it could take a century or more for fresh groundwater to the east to be affected.

The alluvium is unsaturated throughout most of the Midway Valley except for the southeast part of the Midway Valley syncline, the Maricopa depocenter and in the Buena Vista syncline (see highlighted wells in Fig 7b). Where the alluvium contains groundwater in the rest of the Midway Valley, the basal alluvial clay serves as a confining layer and water tables in the alluvium are perched above those in the underlying Tulare Formation (areas circled in red in figure 7b). This behavior was observed in the USGS MSBV monitoring well (32S24E21G01; Fig 7a) drilled in the Midway Valley in 2023 [21].

In many cases, perched water tables in the alluvium are filled with saline water from produced water disposal in ponds or injection wells. The well clusters circled in red in Figure 7b contain water with very low resistivity and chemical analyses from USGS monitoring well MSBV (32S24E21G01) drilled in the Midway Valley in 2023 show that the groundwater salinity is 24,600 mg/L in the alluvial monitoring well [21]. This low resistivity, high salinity water is likely sourced from the disposal of produced water and other waste water allowed to infiltrate from historical disposal ponds located upslope [39] and stream channels used for disposal before about 1955 [7]. This produced water is typically more saline than the native waters in the aquifers into which it is released.

Figure 9 shows a well log cross section superimposed upon a slice from an aerial electromagnetic (AEM) survey obtained in 2018 [40]. The cross section is located downgradient (and down dip) from the southeast Taft produced water disposal ponds. Low resistivity intervals observed in the well logs are denoted by pink bars and generally correspond to red and purple intervals indicating low resistivity on the AEM survey except for MW-1 (32S24E17Q01). Well MW-1 (32S24E17Q01) was completed from 39-52 m (130-170 ft)-- above the low resistivity interval noted in the logs. The open hole logs from 1994 indicate resistivity values of 10-12 ohm-m in the completion interval and samples taken in 1995 show

TDS of 3680 mg/L [41]. The AEM survey from 2018 shows lower resistivity (1-3 ohm-m) over the well's completion interval and sample analyses from the well in 2018 show that TDS ranges from 27,000 - 32,000 mg/L [42]. These data indicate that high salinity produced water, originally filling the lower part of the alluvium, has filled the upper part of the alluvium since 1994.

Fig 9. AEM cross section A-A' along the axis of the Midway Valley syncline.

The location of the AEM cross section is shown in inset map (red line) and in Fig 7b and shows well logs (SP, resistivity and density-neutron—see labels in well 21H) superimposed on aerial electromagnetic survey (AEM) from 2018 [40]. Location of the AEM slice is shown in orange on the inset map. The color scale on the left indicates the resistivity values for the AEM slice. The date each well was drilled and logged is provided at the bottom of the section. Density neutron cross-over (indicating air-filled sands) is shaded in yellow. Water tables (regional (Tulare) and perched) at the time the well was drilled are also shown. Purple and red colors in the AEM indicate low resistivity intervals in 2018. Pink bars in well logs indicate low resistivity salinity anomalies observed in resistivity logs at the time the well was drilled. Produced water disposal ponds from WZI [25] are shown in light blue on the inset map. AEM slice from Ball et al. (2025).

Spatial distribution of groundwater salinity

Generally, the salinity of the groundwater increases with depth from approximately 920 mg/L near the water table in the alluvium in the Yowlumne Oil field in the southeastern part of the study area [11] to over 30,000 mg/L in the Miocene and Pliocene strata [43-45]. Historical chemical analyses suggest that the only saturated sands containing water with less than 10,000 mg/L TDS are the Tulare Formation, the overlying alluvium in the southern and eastern parts of the study area and the Miocene Potter sands of the Monterey Formation in the northwest [43, 46-48, 11]. However, the Potter sands are a major oil reservoir and, as such, are exempt.

The map in Figure 10a shows the depth to 10,000 mg/L to be about 366 m (1,200 feet) in the northwest part of the area. Depth to 10,000 mg/L was also 457 m (1500 ft) or less over the east and west domes of the Buena Vista Oil Field and in a small portion of the southwest Midway Sunset Oil Field. The depth to 10,000 mg/L in the southeastern part of the area is over 1524 m (5000 ft). Four wells have a deeper interval of calculated salinity less than 10,000 mg/L below the upper mapped base of 10,000 mg/L in the southeastern part of the study area and are highlighted by stars in Fig 10a. In all cases, the depth to 10,000 mg/L occurs within the Tulare Formation and, when the Amnicola clay is present, within the lower part of the Tulare Formation.

Fig 10. Maps showing depth to 10,000 mg/L based on calculations and resistivity cutoffs.

Depth to a) 10,000 mg/L (USDW) calculated from Archie's equation using data from 45 wells shown in map and b) 3 ohm-m using data from 560 wells shown in map. Wells denoted with stars contain a deeper interval of groundwater with less than 10,000 mg/L or greater than 3 ohm-m. Contours shown are in feet. Scale shows both metric and US oilfield units (ft).

One drawback to the mapped depth to 10,000 mg/L in Figure 10a is the lack of detail caused by the paucity of wells with log data suitable for Archie's calculations (45 wells were used to construct the map in figure 10a). As a proxy for calculated salinity values, a bulk deep resistivity value of 3 ohm-m from induction resistivity logs was also used to determine the depth at which groundwater salinity reached 10,000 mg/L. The map showing the depth to 10,000 mg/L based on a deep resistivity of 3 ohm-m is shown in Figure 10b and is based on data from 560 wells in the study area (Gannon et al., data release). It bears a strong resemblance to the map in Fig 10a but the increased well control provides more detail. However, without the ability to assign a measured value for porosity at each calculated salinity depth, the depth to 10,000 mg/L is more uncertain in Fig 10b. In seven wells, a deeper interval with resistivity greater than 3 ohm-m is present below the depth where 3 ohm-m was first encountered, implying a

484 deeper zone with lower TDS than 10,000 mg/L in the southeastern part of the study area. These wells
485 are starred in Figure 10b.

486 Changes in groundwater salinity through time

487 The Buena Vista and Midway-Sunset Oil Fields have produced 1.75 billion m^3 (11 billion barrels) of
488 produced water since 1910 [15]. Prior to about 1955, most of this water was discharged to the surface
489 using percolation and evaporation ponds or by allowing it to flow down dry stream channels where it
490 infiltrated into the alluvium [7]. Currently, most disposal occurs as underground injection via water
491 disposal (WD) wells although some surface percolation ponds are still active. Most disposal wells inject
492 produced water into the Tulare Formation in both the saturated and unsaturated zones. Several WD
493 wells also inject into the alluvium in the southern part of the Midway-Sunset oil field however,
494 infiltration of saline water from produced water disposal ponds affects the alluvium in many parts of the
495 study area.

496 Resistivity logs can also be used to determine the extent to which disposal of produced water by
497 infiltration ponds or injection has affected the aquifers provided that the disposed water has a higher
498 salinity than the native waters in the aquifer used for disposal [49,50]. Salinity of disposal pond water
499 ranges from 14,500 to 26,892 mg/L TDS [39] and is much higher than the salinity of the native
500 groundwater near the surface. The changes in resistivity observed in affected, or potentially affected,
501 resistivity logs are termed resistivity anomalies and usually appear as sand intervals near the water table
502 with lower resistivity than that of surrounding sands (Fig 9). If the saline water was injected into the
503 vadose zone, intervals of low resistivity perched water occur between intervals characterized by high
504 resistivity, air-filled sands. The affected sands will also show little or no crossover on density-neutron
505 logs compared to unaffected sands (Fig 11a). In the study area, the saline water from infiltration ponds
506 often perches on the basal alluvial clay where it is present and fills the sands in the alluvium over time as

shown in the logs in figure 7a and the cross section in Figure 9. Wells with noted resistivity anomalies are available in the accompanying data release [11].

Fig 11. Examples of resistivity anomalies caused by produced water disposal.

Examples of resistivity anomalies in the study area from produced water disposal in a) the vadose zone and b) the saturated zone. Deep resistivity above 3 ohms is shaded yellow and density neutron cross-over (denoting sands above the water table) are also shaded yellow. Pink highlighted intervals denote resistivity anomalies. The date the well was drilled and logged is shown below the well log. The well locations are shown as stars in figure 10a. The wells in both Fig 11a and 11b are 60 feet apart but drilled and logged at different times. a) salinity anomalies resulting from produced water disposal within the vadose zone in well 03038915 drilled in 2009. Note the lower resistivity and lack of prominent cross over relative to well 02964099 drilled in 1981. b) Salinity anomalies below the water table are apparent as low resistivity intervals (< 3 ohm-m) in well 02975577 drilled in 1985 after 11 years of produced water disposal in adjacent well 02949650. Note the much lower deep resistivity in this well relative to the original WD well (02949650) drilled in 1974. Black arrows point to sands in which higher resistivity brackish water overlies lower resistivity saline water within individual sands. SP = spontaneous potential log measured in millivolts. Shallow res = shallow resistivity log measured in ohm-m. Deep res = deep resistivity log measured in ohm-m. Neutron = neutron porosity and density = density porosity. The blue well symbol above each well denotes water disposal well.

Where saline water is injected into saturated parts of the aquifer via water disposal wells, the affected intervals exhibit lower resistivity than observed in overlying and underlying sands or have lower resistivity than in nearby older wells drilled prior to the initiation of disposal activities (Fig 11b). When the affected well is close to a source of saline water injection, the saline waters have not had the

opportunity to thoroughly mix with the native waters in the aquifer and, due to the greater density of the saline injectate, the deep resistivity is lower near the bottom of the affected sands than near the top (Fig 11b). At greater distances from the source of injection, or if a long period of time has elapsed between cessation of water disposal and the drilling of the affected well, the stratification of fluids within the sand is less noticeable. This usually manifests as sands that have markedly lower resistivity than underlying sands. These intervals stand out because resistivity tends to decrease with depth as salinity naturally increases with depth.

Figure 12a shows the location of disposal infiltration ponds and injection wells within the study area and Figure 12b shows wells with resistivity anomalies, the earliest year the resistivity anomalies were noted and the probable cause of the anomalies. Most of the affected wells lie near disposal ponds (red) or areas containing high densities of WD wells (blue). However, logs from other wells display resistivity anomalies but are not located near disposal zones or the anomalies pre-date the initiation of water disposal by injection (yellow). The cause of these anomalies is less obvious than those observed in wells near disposal facilities. However, the Midway Valley area contains numerous old wells that were drilled, completed and abandoned in the early decades of the 1900's when well construction and abandonment methods were not as stringent as they are today. Rintoul [51] notes that California's oil sands are often poorly consolidated and interbedded with water sands. Poor construction and abandonment techniques and lack of regulation in the early years of drilling often allowed water from adjacent sands to move behind the well casings into the oil-producing sands causing the producing zones to "water-out" prematurely. This resulted in drastically curtailed oil production in many areas as well as numerous lawsuits between oil companies operating on adjacent leases [51].

Figure 12. a) location of produced water disposal (WD) by injection (circles) colored by year of injection and surface ponds (light blue polygons) noted in Davis et al. [14] and WZI [25]. Year of earliest injection into the Tulare noted near WD well clusters. Red text indicates injection into

555 alluvium as well. Iwr = injection into lower Tulare only. Stars show the location of the wells in
556 Figure 11. b) wells with resistivity anomalies color coded by probable cause. Year of the
557 earliest resistivity anomalies related to disposal activities (ponds or injection) noted next to each
558 WD well cluster. Red text indicates resistivity anomalies in alluvium as well as Tulare. Age of
559 resistivity anomalies of unknown origin are not noted on the map. Note location of cross section
560 shown in Figure 15.

561 Attempts to regulate well construction and abandonment resulted in the establishment of the
562 Department of Petroleum and Gas of the State Mining Bureau in 1915 (later renamed the California
563 Division of Oil and Gas (DOGGR) and, still later, the California Geologic Energy Management Division
564 (CalGEM)). Wells could not be drilled without first notifying the Department which then required the
565 operator to perform a successful water shut off test by cementing the annulus between the well casing
566 and the borehole wall so that water could not flow between the producing zone and the adjacent water
567 sands. These rules were adopted largely to protect the producing zones. The first annual report of the
568 California state oil and gas supervisor describes numerous ways in which water entry into the oil zone
569 can occur due to mechanical well failures [52]. The intermediate well casings above the producing
570 zone—known as the "water string"—often lacked sufficient cement behind pipe to seal the
571 intermediate casing all the way to the surface casing. This allowed water to move behind pipe in the
572 interval of the intermediate casing where there was no cement between the casing and borehole wall.
573 In addition, the casing strings often developed mechanical issues such as holes and crooked or collapsed
574 zones. Figure 13 shows the number of wells examined in this study (approximately 2400) and the
575 number of those wells with mechanical integrity issues grouped by decade drilled. Most wells with
576 mechanical issues were drilled prior to 1930.

577 **Fig 13. Wells with mechanical issues grouped by decade drilled.**

Well histories from 2400 wells in the study area were examined for mechanical issues. The charts show a) the decade in which the wells were completed and b) the number of wells with mechanical problems grouped by the decade in which the wells were completed. A list of the wells included in this table is available in the data release. The locations of the wells with mechanical problems are shown in figure 14.

Mechanical problems are most likely to be discovered quickly in injection wells (both water disposal wells and wells drilled for enhanced oil recovery (EOR)) which are required to be tested regularly to ensure casing integrity. In producing wells, the problems may persist for longer periods of time if they do not adversely affect production. In some cases, the operators were not aware of the problems until the well was reworked or abandoned. This is especially true in the case of marginal producers or idle wells. The cost of repairing mechanical problems in these wells can be prohibitive and mechanical issues could persist for years before the well is repaired or abandoned. These wells are/were potential conduits for the movement of water between various sands above the producing zone—in some cases possibly allowing saline water from deeper sands to enter sands containing fresh or brackish water.

The map in Figure 14 shows approximately 500 wells (highlighted in red) in the study area with mechanical issues noted in well histories. These wells are available in the accompanying data release [11]. This is not an exhaustive list as only about 2400 well histories of the approximately 33,700 wells in the study area were examined. The prevalence of wells with mechanical problems throughout the area may explain the occurrence of resistivity anomalies present in wells drilled and logged prior to or far from water disposal facilities—particularly if the resistivity anomalies occur within the saturated interval and not near the surface where they could be caused by infiltration of produced water from ponds or dry creek beds.

Fig 14. Location of wells with mechanical issues.

Approximately 2400 well histories in the study area were examined for this report. The wells highlighted in red (~500 wells) have mechanical issues noted in their well histories in the CalGEM Wellstar database.

One example of possible salt water intrusion from a well with mechanical problems is shown in the cross section in Figure 15. The resistivity anomalies in three wells occur within the Tulare Formation at depths ranging from 201 to 285 m (660 to 936 ft) and become apparent in nearby well logs in the area as early as 1962. At that time, only one WD well was active in the area. It was located about 1.5 km (1 mi) to the south and began injecting into the alluvium in 1959 in order to determine if subsurface injection would mitigate land subsidence caused by percolation of waste water in sumps. The well ceased injection in 1977. Because its injection was above the alluvial clay confining layer that separates the alluvium from the Tulare aquifer, it is unlikely that it could be the cause of the resistivity anomalies in the underlying Tulare Formation. In addition, wells drilled in 1962 between the WD well and the wells near the cross section in figure 15 do not show any resistivity anomalies. The most likely cause is well 02919352 – near the center of the cross section in figure 15 and only 145 m (475 ft) from the nearest early 1960s well containing the resistivity anomaly. Well 02919352 was drilled and completed in 1936 and was plugged back to reduce water entry in 1957. The well produced only water (40-55 m^3/day or 250 to 350 bbl/day rate) through March 1958 when it was shut in. The well remained shut in until 1982 when testing determined casing leaks at various intervals from 152 to 705 m (501 to 2314 feet). The leaks were not repaired at that time and the well was finally abandoned in 1985.

Fig 15. Cross section showing wells with resistivity anomalies possibly due to well mechanical failure.

Cross section through wells with resistivity anomalies below the water table >~1.5 km (~1 mi.) from produced water disposal wells or ponds. The anomalies may be caused by a well integrity issue in well 02919352 near the center of the cross section. Resistivity anomalies are shown by

pink bars on the log track and are annotated with depth (in ft). An example of the resistivity anomaly in well 02909222 is shown in the upper right corner of the figure and highlighted in pink. The low resistivity interval occupies the lower part of the sand. Mechanical integrity issues are shown by red bars on the log tracks. Date well was drilled is noted at the bottom of the log. Cross section location is shown in inset map in lower right and in Fig 13b. Wells with resistivity anomalies are highlighted in pink on the inset map. WD wells and ponds are shown in blue on the map and oil wells are shown in green. The only WD well (02936091) injecting prior to 1963 is shown by a star in the inset map.

Discussion and Conclusions

The Midway Valley study area contains important oil and gas-producing fields—especially the giant Midway-Sunset field—the largest oil-producing field in California in 2021. Groundwater in the area is generally brackish. Groundwater containing less than 10,000 mg/L TDS is one of the criteria considered for an aquifer zone to be designated as an Underground Source of Drinking Water under federal regulations. The area within the administrative boundaries of the oilfields within the study area is primarily designated as exempt, not serving as a source of drinking water and allowed to be used for oil extraction and disposal, but the eastern and southeastern parts of the study area contain groundwater that is less than 10,000 mg/L and is not exempt.

The major aquifers in the area are the Tulare Formation and the overlying alluvium. Both aquifers were deposited in fluvial and lacustrine environments, but the Tulare contains thicker, more numerous sand layers than the overlying alluvium. In the west, along the basin margin, the aquifers are separated by an unconformity but, farther east near the basin axis, the contact becomes more conformable and the contact between the aquifers becomes more difficult to ascertain on geophysical logs. Likewise, in the west, the sand-rich Tulare Formation unconformably overlies the marine San Joaquin Formation in

which sands are separated by thick marine clays. However, farther east, the clays of the San Joaquin Formation are replaced by a thick sequence of discontinuous sands that are indistinguishable from those in the overlying Tulare Formation on the electrical logs. Here, both formations are mapped as a single entity termed the Tulare lithosome. The combined alluvium/Tulare lithosome reaches a thickness of up to 2438 m (8000 feet) in the southeast part of the study area in the basin axis.

The water table within the alluvium/Tulare aquifer in the study area slopes to the east. Geophysical logs show that salinity increases with depth and the depth to a salinity of 10,000 mg/L lies at a depth of about 366 m (1200 feet) in the northwest and 1524-1829 m (5000-6000 feet) in the southeast. The western part of the study area within the oil-field boundaries contains numerous sumps and injection wells used to dispose of saline produced water within the aquifers. Changes in resistivity in logs drilled near the disposal areas during different time periods show that the salinity of some of the saturated sands has increased over time in these areas and some parts of the unsaturated zone now contain perched saline water. Other wells containing intervals of low resistivity within intervals of overall higher resistivity, termed resistivity anomalies, are observed in areas not associated with produced water disposal. The study area contains numerous wells drilled in the early decades of the 1900's when well construction standards were less stringent than they are today. Mechanical failure in these old, poorly constructed or abandoned wellbores may be the cause of the resistivity anomalies in wells that are not adjacent to water disposal areas—particularly when the resistivity anomalies occur within saturated intervals.

Acknowledgements

This work was primarily funded by the California State Water Resources Control Board Oil and Gas Regional Monitoring Program. Advice and editing from Matt Landon of the US Geological Survey is greatly appreciated.

References

1. Kern Economic Development Foundation. The economic contribution of the oil and gas industry in Kern County. 2021 [cited 2025 Apr 15]; Available from: kernedc.com/wp-content/uploads/2021/04/KEDF-Economic-Contribution-of-the-Oil-and-Gas-Industry-in-Kern-County_-2021.pdf.
2. Enverus. Top Producing Counties/areas 2013. 2013 [cited 2025 Jun24]; Available from: www.enverus.com/blog/half-us-oil-production-comes-20-counties/.
3. KGET. Kern County is the top agricultural producer in nation. 2022 [cited 2025 Jun 25]; Available from: www.kget.com/news/state-news/kern-county-is-the-top-agricultural-producer-in-nation/.
4. Water Association of Kern County. Water in Kern County. 2025 [cited 2025 Jun 25]; Available from: www.wakc.com/water-overview/kern-county/.
5. California Department of Water Resources. California's Groundwater (Bulletin 118). 2020 [cited 2025 Apr 15]; Available from: water.ca.gov/Programs/Groundwater-Management/Bulletin-118.
6. Faunt CC. ed. Groundwater availability of the Central Valley Aquifer, California: U.S. Geological survey Prof. Paper 1766. 2009.
7. Gannon R, Landon MK, Kulongoski JT, Stephens MJ, Ball LB, Warden JG, Davis TA, Gillespie JM, and Cozzarelli IM. Relations of groundwater quality to long term surface disposal of produced water near the Midway-Sunset and Buena Vista Oil Fields, California, USA. Science of the Total Environment. 2025 [cited 2025 Sept 23]; Available from: https://doi.org/10.1016/j.scitotenv.2025.179637.
8. Bartow JA. The Cenozoic evolution of the San Joaquin Valley, California. USGS Prof. Paper 1501 1991: 40 p.

9. Quinn MJ. 1990, Upper Miocene Stevens sands in the Maricopa Depocenter, southern San Joaquin Valley, California. In: Kuespert JG and Reid SA, editors. Structure, Stratigraphy and Hydrocarbon Occurrences of the San Joaquin Basin, California: 1990 [cited 2025 Sept 23]; The Pacific Section Am. Assn. of Petroleum Geologists Spec Pub No 64p. 97-113. Available from: https://doi.org/10.32375/1990-GB65.
10. Atwater TM. Implications of plate tectonics for the Cenozoic tectonic evolution of western North America. Geol. Soc. Am. Bull. 1970;81:3513-3536.
11. Gannon RS, and Gillespie JM. in review, Geophysical, geological, hydrological, and geochemical data for the Midway Valley study area, southwestern Kern County, California. U.S. Geological Survey Data Release. Forthcoming.
12. CalGEM. Annual Report 2021, California State Oil and Gas Supervisor Annual Report 2021. 2024[cited 2025 Feb 7]: Available from: California State Oil and Gas Supervisor Annual Report 2021.
13. CA DOGGR. California oil and gas fields volume 1—central California. Sacramento (CA): California Dept. of Conservation, Div. of Oil, Gas and Geothermal Resources: 1998.
14. Davis TA, Gannon RS, Warden JG, Rodriguez O., Gillespie JM, Ball LB, Qi SL, and Metzger LF. Produced water disposal at percolation and evaporation ponds in and near oil fields in the southwestern San Joaquin Valley, California (Data Release; ver. 2.0, October 2024). U.S. Geological Survey. 2024 [cited 2025 Sept 23]; Available from: https://doi.org/10.5066/P999XIP9
15. California Department of Conservation. *Oil and gas online data: Geologic Energy Management Division*. 2023 [cited 2025 Jan 28]. Available from: https://www.conservation.ca.gov/calgem/Pages/WellFinder.aspx.
16. Scheirer AH and Magoon LB. Age, distribution and stratigraphic relationship of rock units in the San Joaquin Basin Province, California. In: Scheirer AH and Magoon LB, editors. Petroleum

718 Systems and Geologic Assessment of Oil and Gas in the San Joaquin Basin Province, California:
719 US Geological Survey Professional Paper 1713, Ch. 5; 2007 [cited 2025 Sept 23]. Available from:
720 https://pubs.usgs.gov/pp/pp1713/05/pp1713_ch05.pdf.
721 17. Pisciotto KA and Garrison RE. Lithofacies and depositional environments of the Monterey
722 Formation, California. In: Garrison RE and Douglas RG, editors. The Monterey Formation and
723 related Siliceous Rocks of California: Pac Sec. SEPM Spec Pub; 1981. p. 97-122.
724 18. Murer AS, McClennen KL, Ellison TK, Larson DC, Timmer RS, Thomsen MA and Wolcott KD.
725 Steam injection project in heavy-oil diatomite: Soc. Pet Eng. Paper 38302. 2000.
726 19. Reid SA. Miocene and Pliocene depositional systems of the southern San Joaquin basin and
727 formation of sandstone reservoirs in the Elk Hills area, California. In: Fritsche AE, editor.
728 Cenozoic Paleogeography of the western United States—II. Pacific Section Soc. of Economic
729 Paleontologists and Mineralogists book 75, 1995. p. 131-150.
730 20. Nilsen TH. Regional geology of the southwestern San Joaquin Basin, California. In: Nilsen TH,
731 Wylie AS Jr. and Gregory GJ, Editors. Geology of the Midway-Sunset Oil Field: American
732 Association of Petroleum Geologists Field Trip Guidebook. Pacific Section American Assn. of
733 Petroleum Geologists. 1996; p. 7-38.
734 21. Everett RR, Gillespie JM, Gannon RS, Brown AA, and Morita AY. in review, Multiple-well
735 monitoring site adjacent to the Midway-Sunset and Buena Vista Oil Fields, Kern County,
736 California: USGS Scientific Investigations Report, Forthcoming.
737 22. Dibblee TW and Minch JA. Geologic map of the Maricopa and Pentland quadrangles, San Luis
738 Obispo and Kern counties, California. Dibblee Geological Foundation Map DF-94, 1:24,000.
739 2005a [cited 2025 Feb 14]; Available from: https://ngmdb.usgs.gov/mapview.

740 23. Dibblee TW and Minch JA. Geologic map of the Taft and mouth of the Kern quadrangles, Kern
741 County, California: Dibblee Geological Foundation Map DF-95, 1:24,000. 2005b [cited 2025 Feb
742 14]; Available at: https://ngmdb.usgs.gov/mapview (accessed 2/14/2025).
743 24. Dibblee TW and Minch JA. Geologic map of the Fellows quadrangle, Kern and San Luis Obispo
744 counties, California. Dibblee Geological Foundation Map DF-96. 1:24,000. 2005c [cited 2025 Feb
745 14]; Available from: https://ngmdb.usgs.gov/mapview.
746 25. WZI. Valley Waste Disposal Company, Hydrogeology and Disposal of Oil Field Wastewater,
747 Southwest Kern County, Phase I, January 1988. 1988 [cited 2022 July 5]; Available from:
748 https://geotracker.waterboards.ca.gov/view_documents?global_id=L10004301387&document_
749 id=6039693.
750 26. Bean RT and Logan J. Lower Westside water quality investigation, Kern County: prepared for
751 California State Water Resources Control Board under contract No. 2- 096-158-0. 1983.
752 27. Ball LB, Davis TA, Minsley BJ, Gillespie JM, and Landon MK. 2020, Probabilistic categorical
753 groundwater salinity mapping from airborne electromagnetic data adjacent to California's Lost
754 Hills and Belridge oil fields. *Water Resources Research* 2020 [cited 2025 Sept 23];56. Available
755 from: https://doi.org/10.1029/2019WR026273
756 28. Mitchell DC. The effects of oilfield operations on underground sources of drinking water in Kern
757 County: Sacramento, CA: California Department of Conservation Division of Oil and Gas Pub. No.
758 TR36; 1979.
759 29. Gillespie J, Kong D, and Anderson SD. Groundwater salinity in the southern San Joaquin Valley.
760 AAPG Bull. 2017; 101(8):1239–1261. Available from: https:// doi. org/ 10. 1306/ 09021 616043.
761 Subscription required.

30. U.S. Environmental Protection Agency. EPA oversight of California's Underground Injection Control (UIC) Program. 2024 [cited 2025 Mar 17]; Available from: https://www.epa.gov/uic/epa-oversight-californias-underground-injection-control-uic-program.
31. California Department of Conservation. Aquifer exemptions. 2025; Available from: https://www.conservation.ca.gov/calgem/Pages/Aquifer_Exemptions.aspx. (accessed March 17, 2025)
32. CA DOGGR. California Oil and Gas Fields, vol. 1, North and East-Central California, Sacramento, CA. 1973 [cited 2025 May 5]; 667 p. Available from: www.conservation.ca.gov/calgem/general_information/Documents/Volume%20I%201973%20North%20and%20East%20Central%20California%20Version.PDF.
33. Archie GE. The electrical resistivity log as an aid in determining some reservoir characteristics. Am. Inst. Min. Metall. Eng. Trans. 1942;**146**:54–62.
34. Winsauer, WO, Shearin HM, Masson PH and Williams M. Resistivity of brine-saturated sands in relation to pore geometry. Bull. Am. Assoc. Pet. Geol. 1952;36:253–277.
35. Carothers JE. A statistical study of the formation factor relation to porosity. The Log Analyst. 1968; 9(5): 13-20.
36. CalGEM. 2025 [cited 2025 Jan 27]; Available from: https://filerequest.conservation.ca.gov/WellRecord?api=02959052.
37. Bateman RM and Konen CE. The log analyst and the programmable pocket calculator. The Log Analyst 1977;18(5):3-11.
38. California Department of Water Resources. SGMA Data Viewer. 2025 [cited 2025 Jun 17]; Available from: https://sgma.water.ca.gov/webgis/?appid=SGMADataViewer#currentconditions.

785 39. Geomega Inc. Phase II Groundwater Investigation Report, Valley Waste Disposal Company,
786 Midway Valley - Southeast Taft Area. 2008 [cited 2022 Jun 16]; Available from:
787 https://geotracker.waterboards.ca.gov/profile_report.asp?global_id=T10000013268#sitedocum
788 ents.
789 40. Ball LB, Hoogenboom BE and Zamudio KD. 2025, Airborne electromagnetic and magnetic survey
790 data, southwestern San Joaquin Valley near Maricopa, California, 2018: U.S. Geological Survey
791 data release. 2025[cited 2025 Sept 26]. Available from: https://doi.org/10.5066/P9R1XBPG.
792 41. Kennedy Jenks. Hydrogeologic characterization report, Valley Waste Disposal Company, Midway
793 Valley Study area. 1997 [cited 2025 Mar 1]; Available from:
794 documents.geotracker.waterboards.ca.gov/regulators/deliverable_documents/6766006946/Ma
795 ricopaW_HydroGeo%20rpt%2012-1-97.pdf.
796 42. Golder Associates Inc. Valley Water Management Company South East Taft 2020 Annual
797 Sampling and Analyses Report. 2021 [cited 2022 July 26]; Available from:
798 geotracker.waterboards.ca.gov/profile_report.asp?global_id=T10000013268#sitedocuments.
799 43. Midway-Sunset Oil Field Operators. Midway-Sunset oil field aquifer exemption and expansion
800 application package for Phase 1 deep zones Potter Sands, Spellacy Sands, Miocene shales and
801 Warson Sand, and lower Antelope sands: 2018 [cited 2025 Jun 28]; Available at:
802 www.conservation.ca.gov/calgem/Pages/Aquifer-Exemptions-Status.aspx#midwaysunset.
803 44. Geomega. Hydrogeochemistry Report, southeast Taft area, Valley Waste Disposal Company.
804 2006 [cited 2025 Mar 6]; Available at:
805 documents.geotracker.waterboards.ca.gov/regulators/deliverable_documents/7462602913/4-
806 13-2006%20VWMC_SE%20Taft%20HydroGoeChem%20Rpt_.pdf.
807 45. Gannon RS, Kulongoski JT, and Marcusa JA. Water chemistry data for samples collected at
808 groundwater sites in the Midway-Sunset and Buena Vista Oil Fields study area, March 2018-April

2019, Kern County, California (Data Release). U.S. Geological Survey. 2025 [cited 2025 Sept 23]; Available from: https://doi.org/10.5066/P148AZKG

46. Haugen EA, Finney DMN, Ducart A, Stephens, MJ, and Shimabukuro DH. Geophysical and geochemical data for salinity mapping in the Midway-Sunset oil field area (Data Release). U.S. Geological Survey. 2018 [cited 2025 Sept 23]; Available from: www.sciencebase.gov/catalog/item/5b6a1411e4b006a11f7778c4.
47. Seitz NO, Cozzarelli IM, Gannon RS, Jaeschke JB, Kulongoski JT, Lorah MM, Marcusa JA, and McMahon PB. Produced water chemistry data collected from the Poso Creek, Midway-Sunset, and Buena Vista Oil Fields, 2020-21, Kern County, California: U.S. Geological Survey data release. 2024 [cited 2025 Sept 23]; Available from: https://doi.org/10.5066/P97P2NAN.
48. Metzger LF, Herrera PJ, Rodriguez O, and Gereghty KC. Inorganic chemistry data for groundwater wells near selected oil fields in the southwestern San Joaquin Valley, central California (Data Release). US Geological Survey. 2020 [cited 2025 Sept 23]; Available from: https://doi.org/10.5066/P9XK9AQ1
49. Gillespie JM, Davis TA, Stephens MJ, Ball LB and Landon ML. Groundwater salinity and the effects of produced water disposal in the Lost Hills-Belridge oilfields, Kern County, California: Environmental Geosciences. 2019; 26: 73-96
50. Gillespie JM, Stephens MJ, Chang W, and Warden JG. Mapping aquifer salinity gradients and effects of oil field produced water disposal using geophysical logs: Elk Hills, Buena Vista and Coles Levee Oil Fields, San Joaquin Valley, California. PLOS ONE. 2022 [cited 2025 Sept 23]; 17(3). Available from: https://doi.org/10.1371/journal.pone.0263477
51. Rintoul W. Drilling Through Time. Sacramento, CA: California Division of Oil and Gas Publication TR40; 1990.

52. California State Oil and Gas Supervisor. First Annual Report for fiscal year 1915-16. Sacramento (CA): California State Printing Office; 1917.

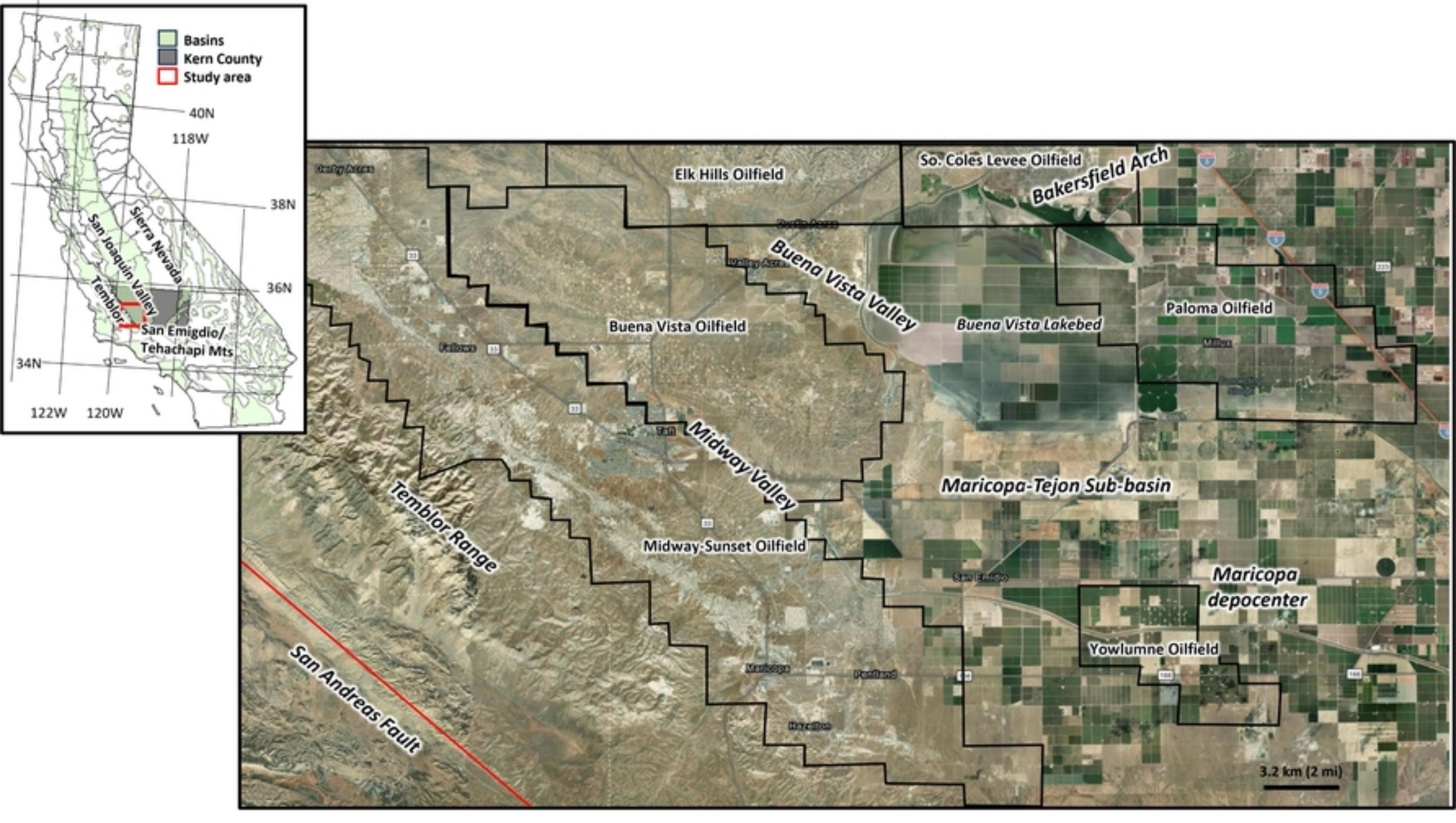
Basins
Kern County
Study area
40N
118W
38N
36N
34N
122W
120W
Sierra Nevada
San Joaquin Valley
Temblor
San Emigdio/
Tehachapi Mts
Elk Hills Oilfield
So. Coles Levee Oilfield
Bakersfield Arch
Buena Vista Valley
Buena Vista Oilfield
Buena Vista Lakebed
Paloma Oilfield
Midway Valley
Temblor Range
Maricopa-Tejon Sub-basin
Midway-Sunset Oilfield
Maricopa
depocenter
Yowlumne Oilfield
San Andreas Fault
3.2 km (2 mi)

Figure

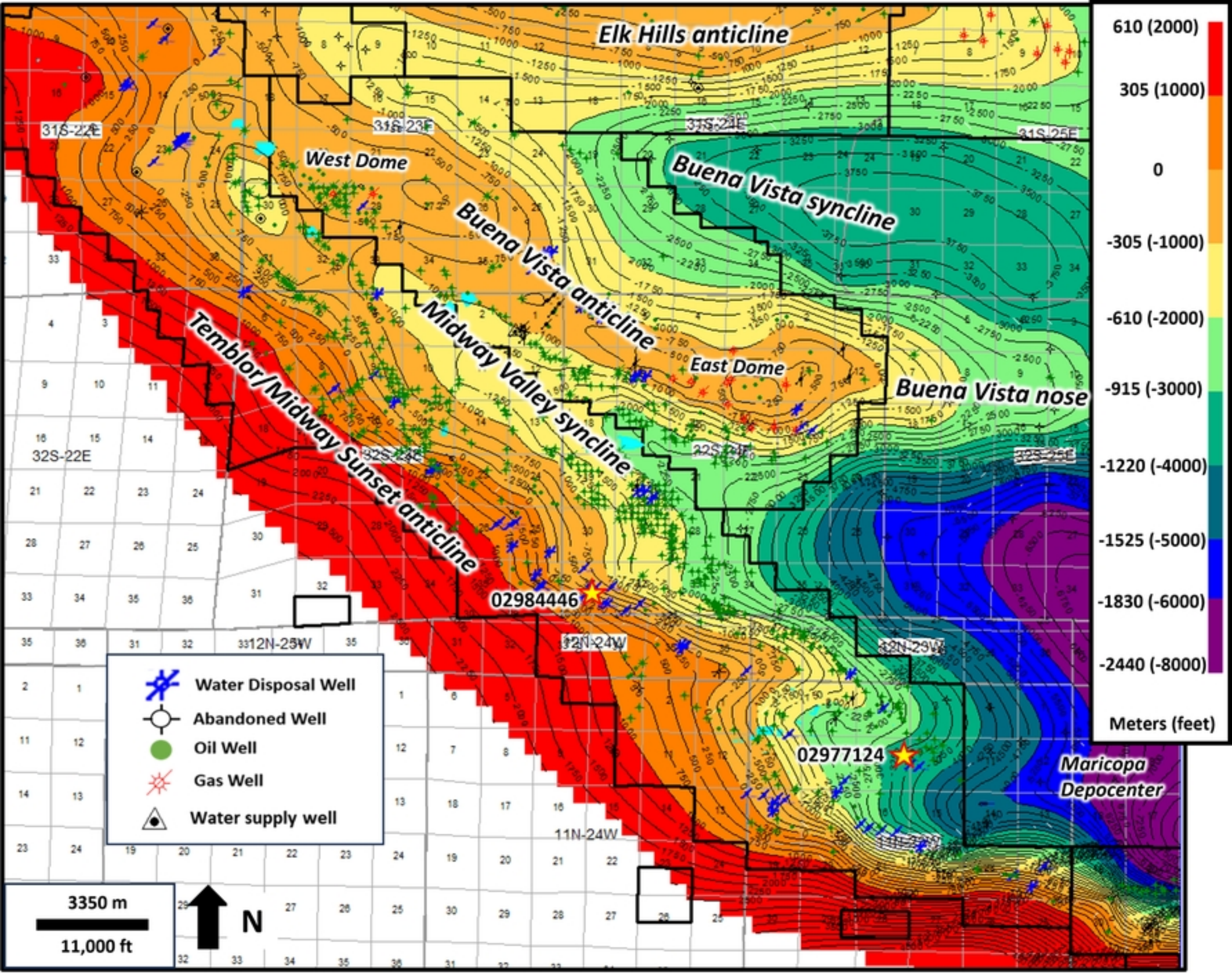
Elk Hills anticline
West Dome
Buena Vista syncline
Buena Vista anticline
Midway Valley syncline
East Dome
Buena Vista nose
Temblor/Midway Sunset anticline
02984446
02977124
Maricopa Depocenter
31S-22E
31S-23E
31S-24E
31S-25E
32S-22E
32S-23E
32S-24E
32S-25E
12N-23W
12N-24W
12N-25W
11N-24W
610 (2000)
305 (1000)
0
-305 (-1000)
-610 (-2000)
-915 (-3000)
-1220 (-4000)
-1525 (-5000)
-1830 (-6000)
-2440 (-8000)
Meters (feet)
Water Disposal Well
Abandoned Well
Oil Well
Gas Well
Water supply well
3350 m
11,000 ft
N

Figure

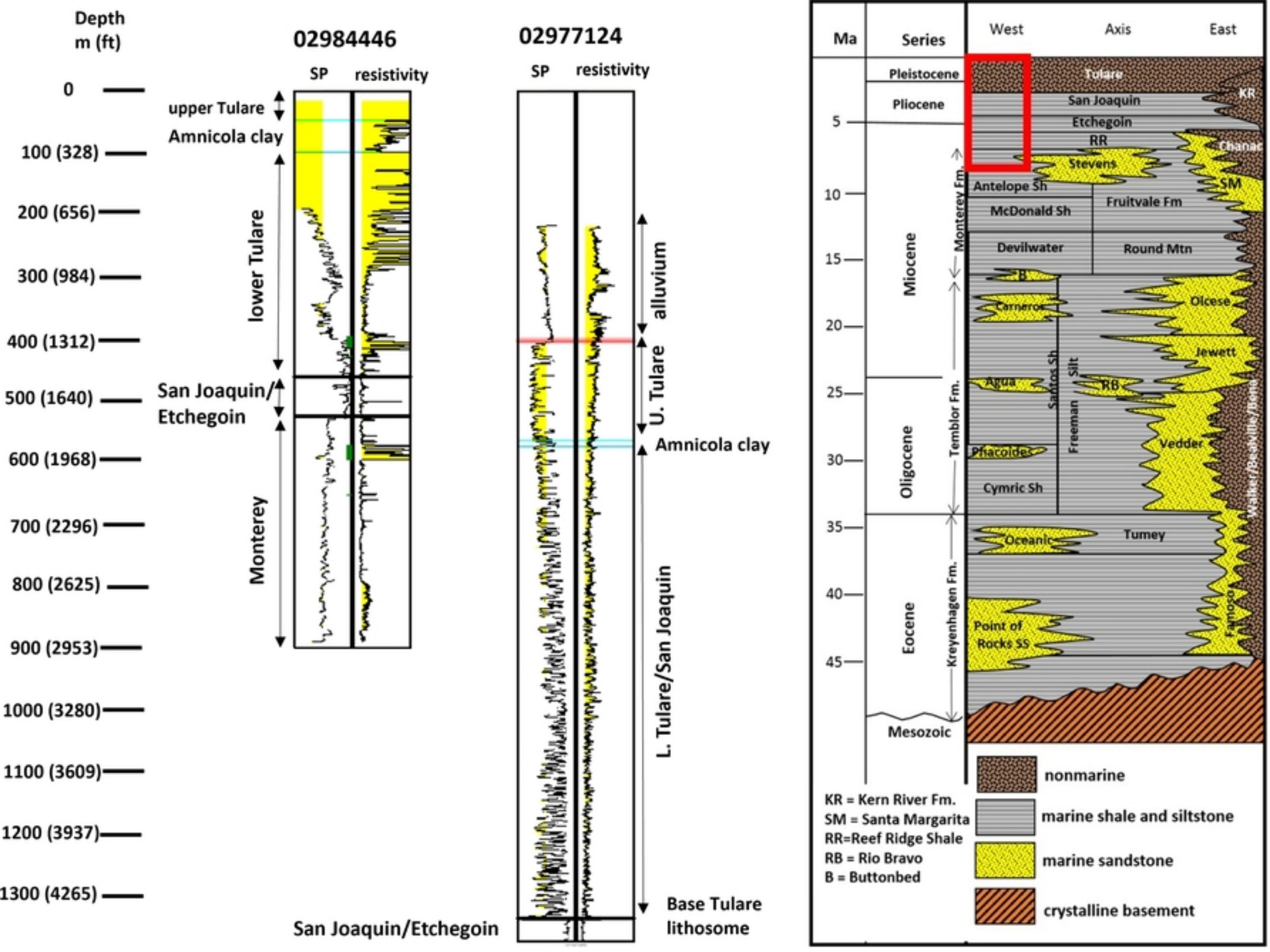
Depth
m (ft)
0
100 (328)
200 (656)
300 (984)
400 (1312)
500 (1640)
600 (1968)
700 (2296)
800 (2625)
900 (2953)
1000 (3280)
1100 (3609)
1200 (3937)
1300 (4265)
02984446
SP
resistivity
upper Tulare
Amnicola clay
lower Tulare
San Joaquin/
Etchegoin
Monterey
02977124
SP
resistivity
alluvium
U. Tulare
Amnicola clay
L. Tulare/San Joaquin
Base Tulare
lithosome
San Joaquin/Etchegoin
Ma
Series
West
Axis
East
Pleistocene
Pliocene
Miocene
Oligocene
Eocene
Mesozoic
Monterey Fm.
Temblor Fm.
Kreyenhagen Fm.
Tulare
San Joaquin
Etchegoin
KR
RR
Chanac
Stevens
SM
Antelope Sh
McDonald Sh
Fruitvale Fm
Devilwater
Round Mtn
B
Carneros
Olcese
Jewett
Agua
Santos Sh
Silt
Freeman
RB
Vedder
Phacoides
Cymric Sh
Walker/Basalt/Famoso
Oceanic
Tumey
Famoso
Point of
Rocks SS
KR = Kern River Fm.
SM = Santa Margarita
RR=Reef Ridge Shale
RB = Rio Bravo
B = Buttonbed
nonmarine
marine shale and siltstone
marine sandstone
crystalline basement

Figure

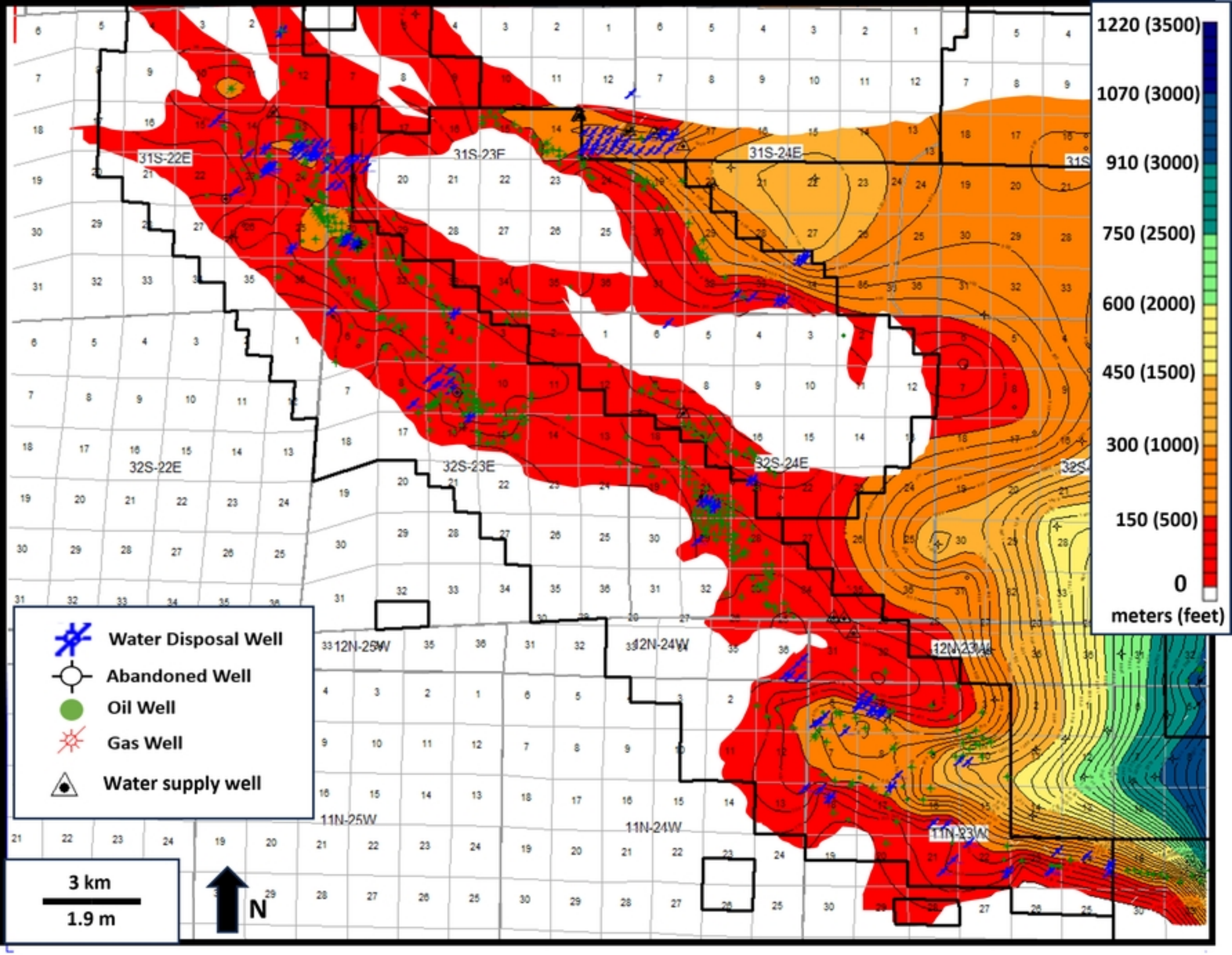
1220 (3500)
1070 (3000)
910 (3000)
750 (2500)
600 (2000)
450 (1500)
300 (1000)
150 (500)
0
meters (feet)
31S-22E
31S-23E
31S-24E
32S-22E
32S-23E
32S-24E
12N-25W
12N-24W
11N-25W
11N-24W
Water Disposal Well
Abandoned Well
Oil Well
Gas Well
Water supply well
3 km
1.9 m
N

Figure

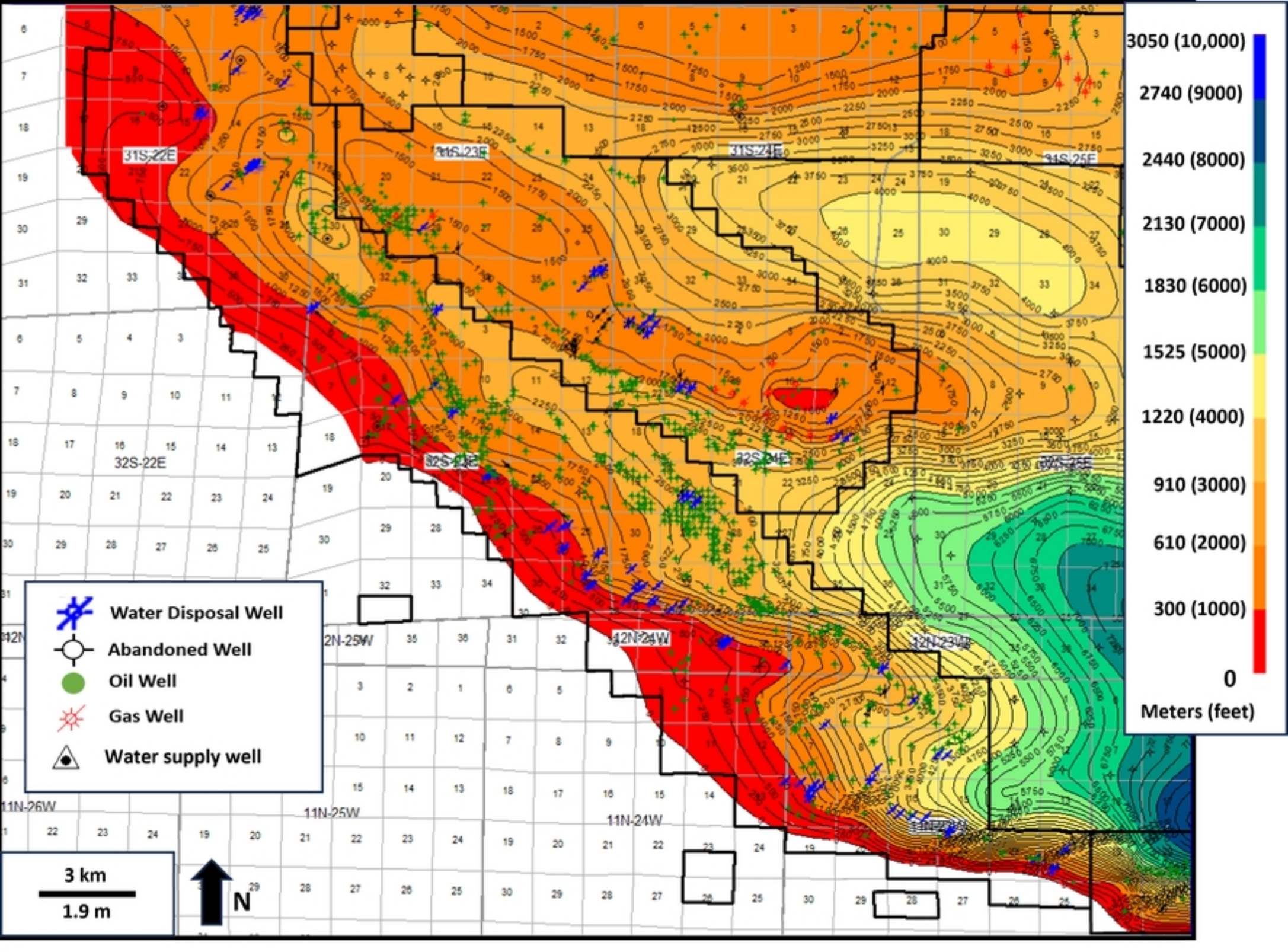
3050 (10,000)
2740 (9000)
2440 (8000)
2130 (7000)
1830 (6000)
1525 (5000)
1220 (4000)
910 (3000)
610 (2000)
300 (1000)
0
Meters (feet)
Water Disposal Well
Abandoned Well
Oil Well
Gas Well
Water supply well
31S-22E
31S-23E
31S-24E
31S-25E
32S-22E
32S-23E
32S-24E
32S-25E
12N-25W
12N-24W
12N-23W
11N-26W
11N-25W
11N-24W
3 km
1.9 m
N

Figure

a. 32S24E21G01 MSBV Midway Valley Syncline

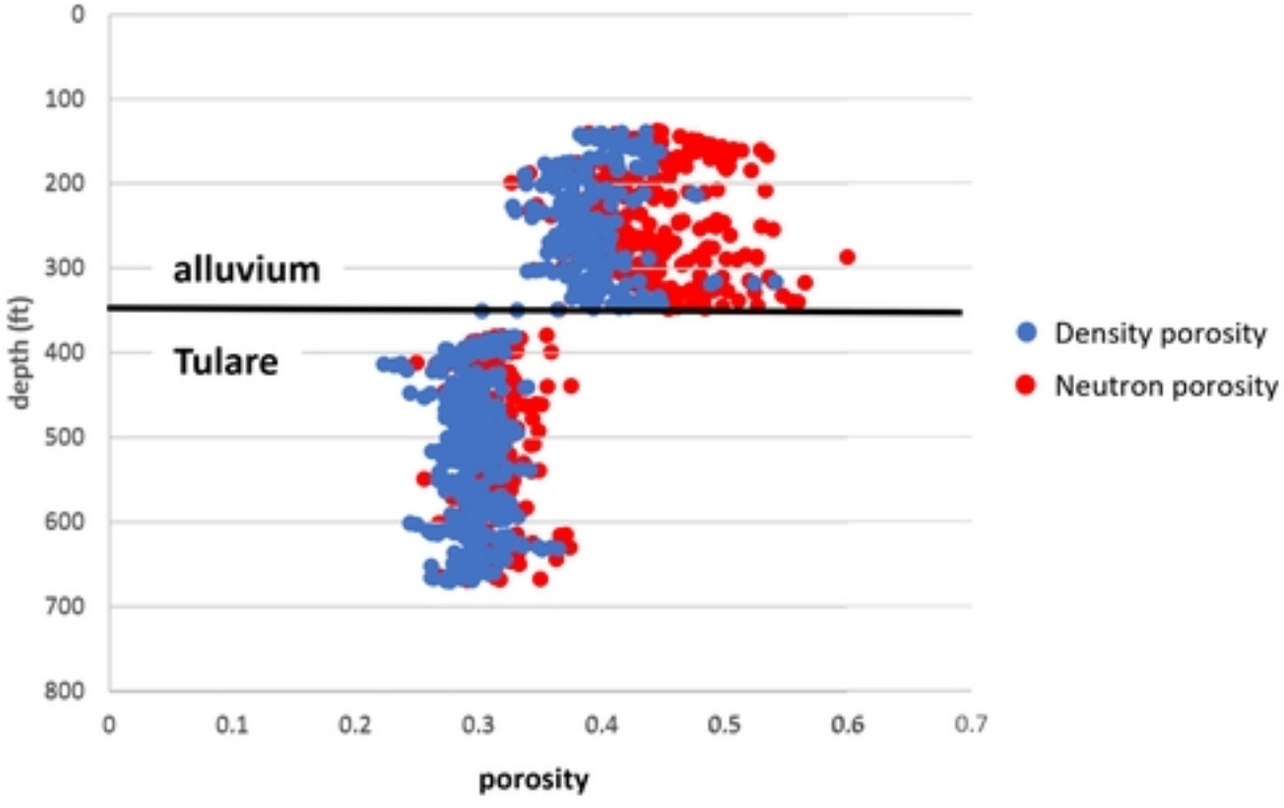

b. 02995001 MW D-1 BV Lakebed

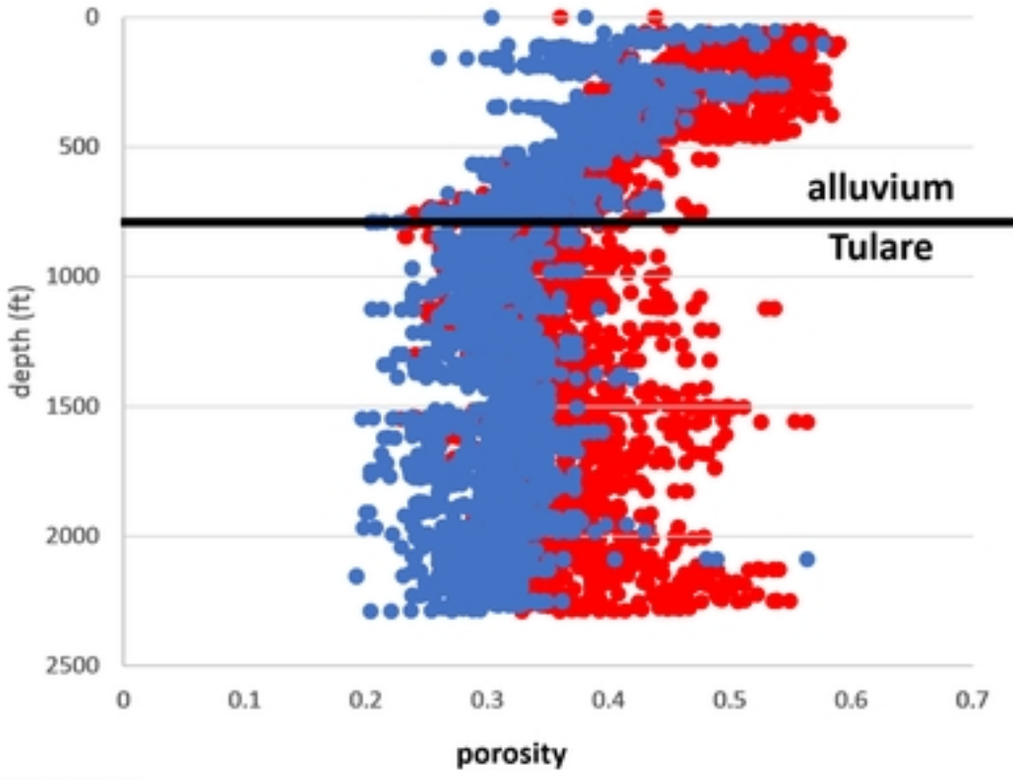

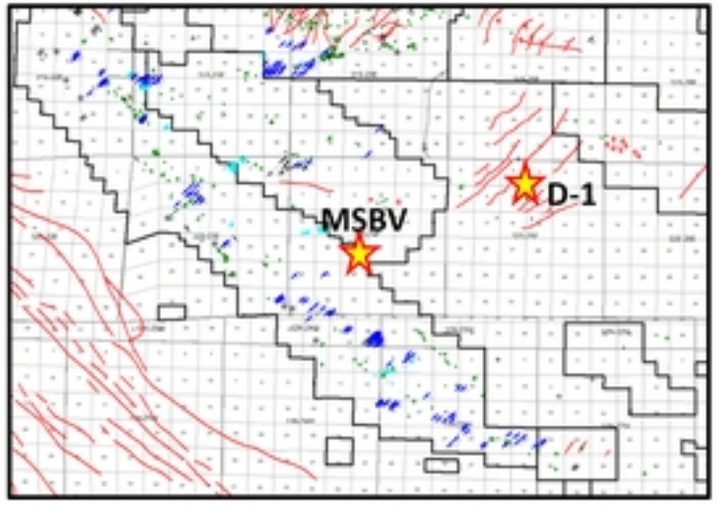

Figure

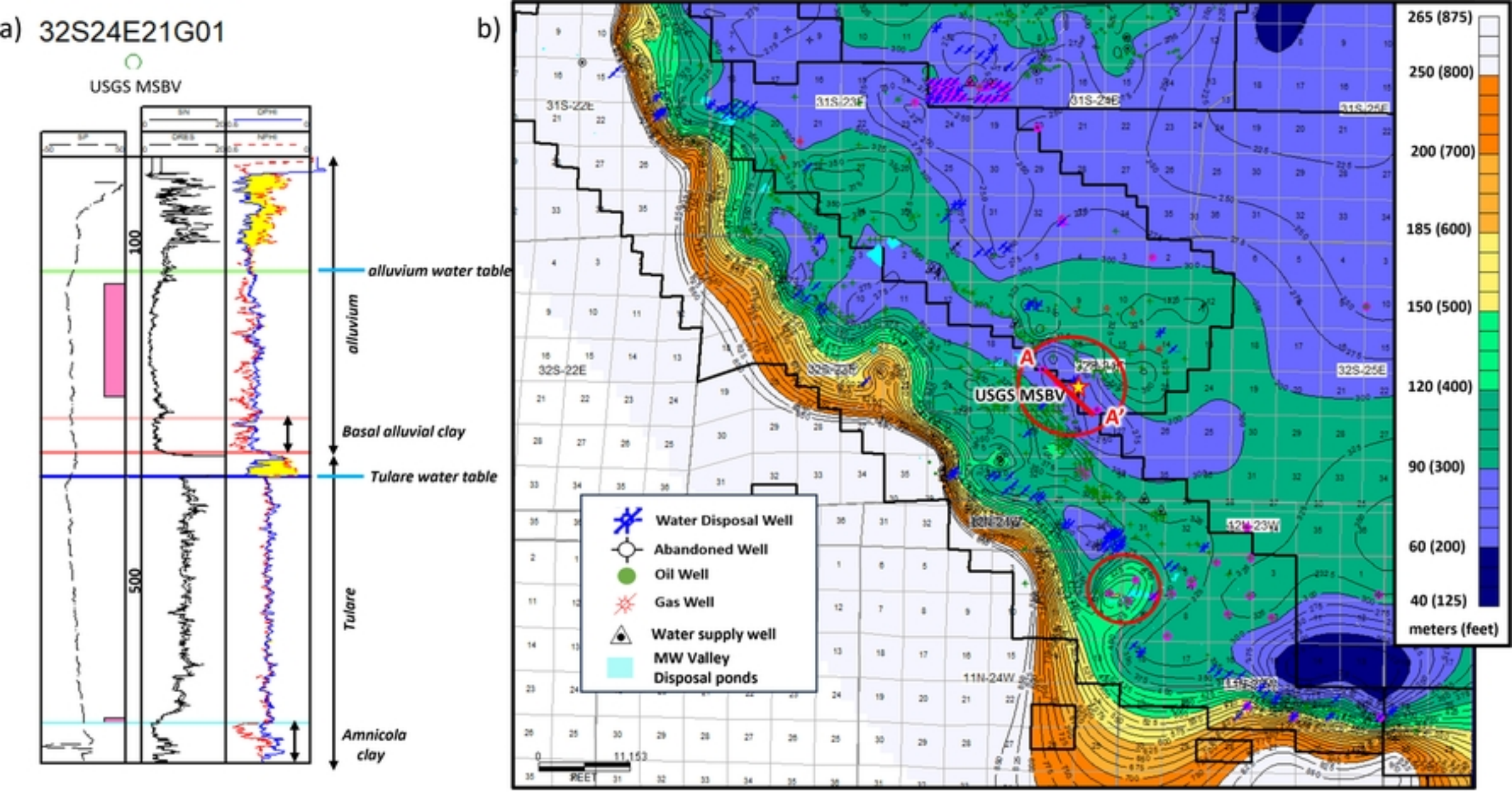
a) 32S24E21G01
USGS MSBV
100
500
alluvium water table
alluvium
Basal alluvial clay
Tulare water table
Tulare
Amnicola clay
b)
A
A'
USGS MSBV
Water Disposal Well
Abandoned Well
Oil Well
Gas Well
Water supply well
MW Valley
Disposal ponds
265 (875)
250 (800)
200 (700)
185 (600)
150 (500)
120 (400)
90 (300)
60 (200)
40 (125)
meters (feet)
31S-22E
31S-23E
31S-24E
31S-25E
32S-22E
32S-25E
12N-23W
12N-24W
11N-24W
0
11,153
FEET

Figure

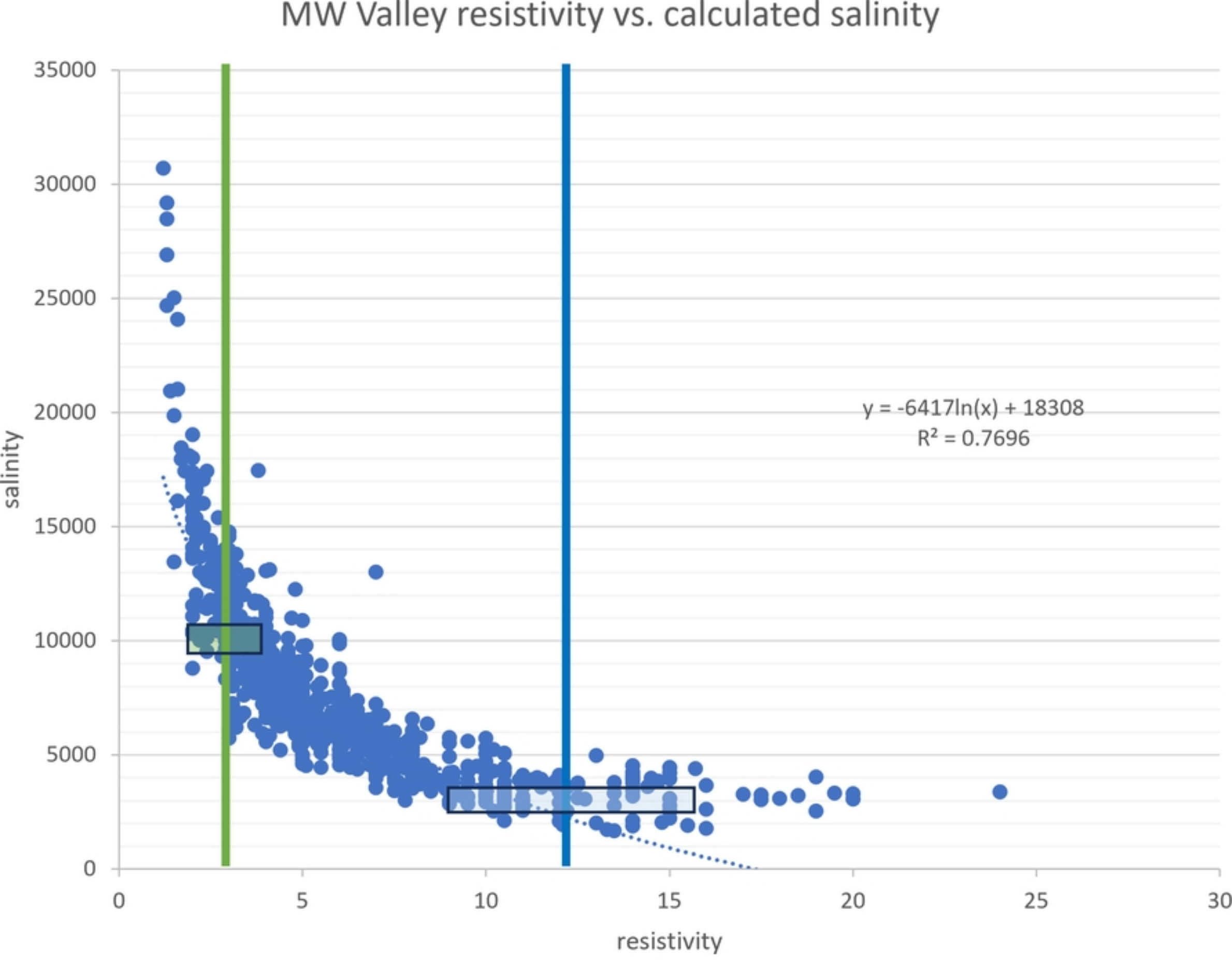
MW Valley resistivity vs. calculated salinity
35000
30000
25000
20000
15000
10000
5000
0
salinity
0
5
10
15
20
25
30
resistivity
y = -6417ln(x) + 18308
R² = 0.7696

Figure

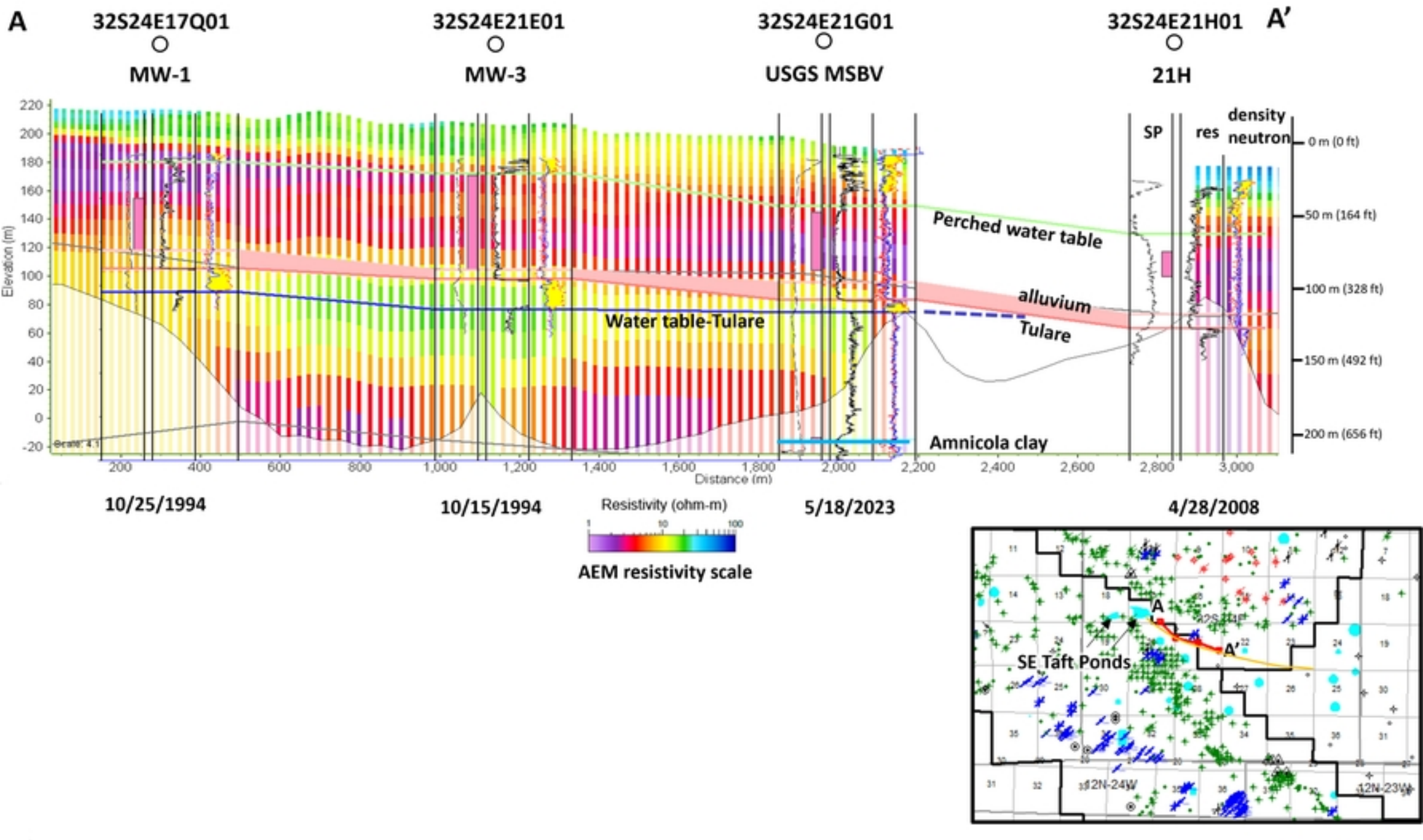
A
32S24E17Q01
MW-1
32S24E21E01
MW-3
32S24E21G01
USGS MSBV
32S24E21H01
21H
A'
SP
res
density
neutron
Perched water table
alluvium
Water table-Tulare
Tulare
Amnicola clay
Elevation (m)
Distance (m)
0 m (0 ft)
50 m (164 ft)
100 m (328 ft)
150 m (492 ft)
200 m (656 ft)
10/25/1994
10/15/1994
5/18/2023
4/28/2008
Resistivity (ohm-m)
AEM resistivity scale
SE Taft Ponds
12N-24W
12N-23W

Figure

a.

b.

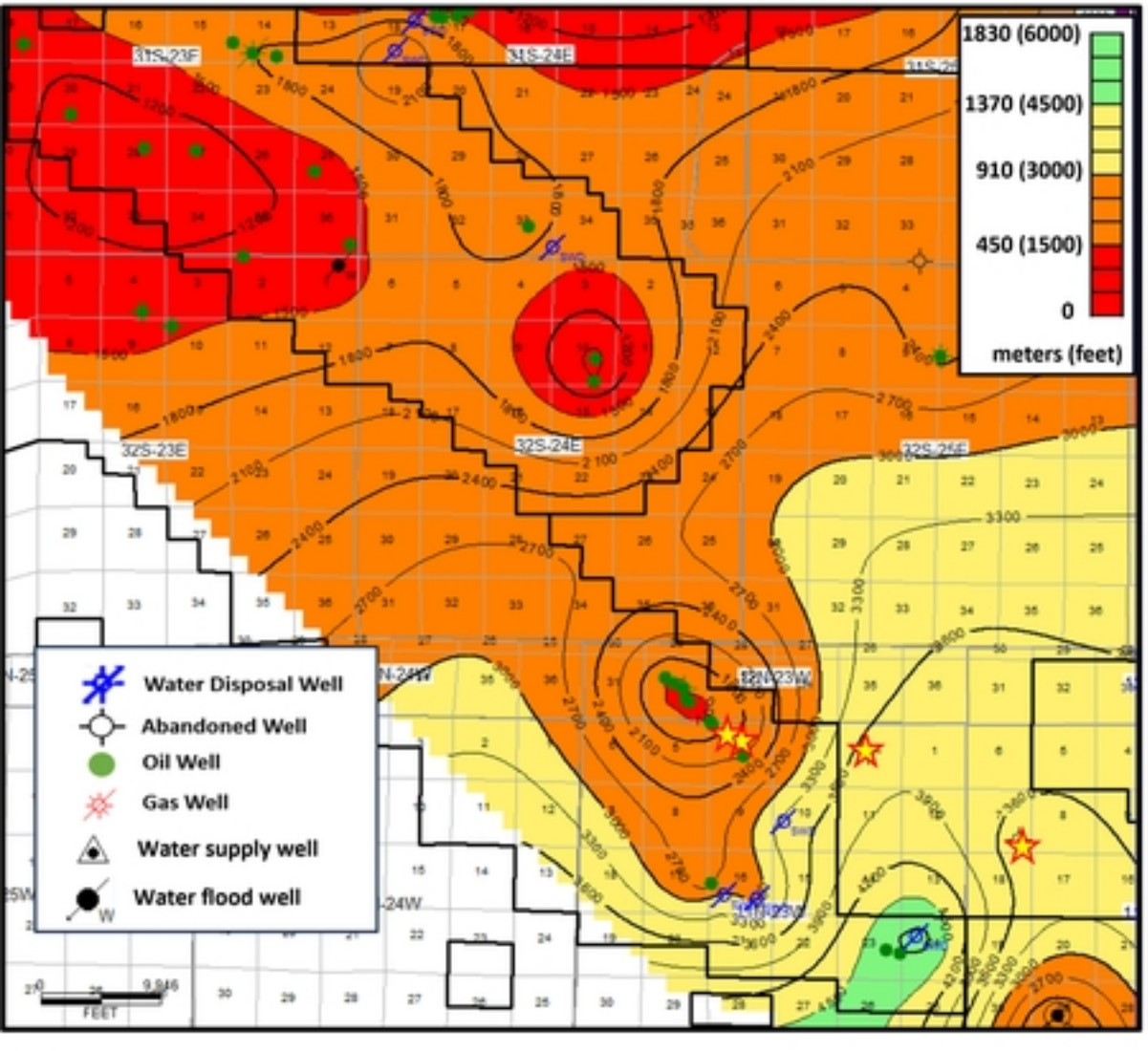
1830 (6000)
1370 (4500)
910 (3000)
450 (1500)
0
meters (feet)
Water Disposal Well
Abandoned Well
Oil Well
Gas Well
Water supply well
Water flood well
31S-23E
31S-24E
32S-23E
32S-24E
12N-23W
FEET

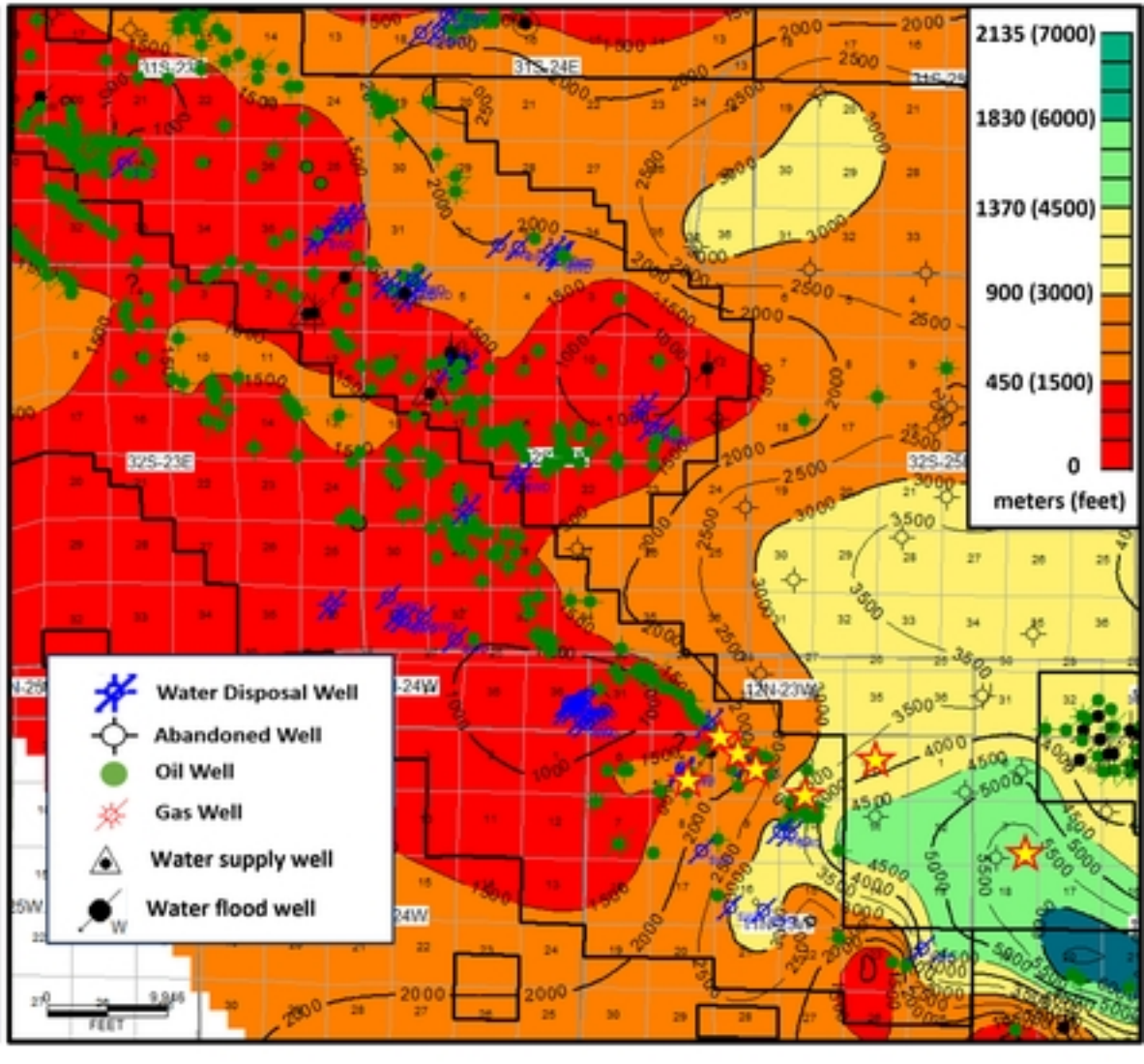
2135 (7000)
1830 (6000)
1370 (4500)
900 (3000)
450 (1500)
0
meters (feet)
Water Disposal Well
Abandoned Well
Oil Well
Gas Well
Water supply well
Water flood well
31S-24E
32S-23E
12N-23W
FEET

Figure

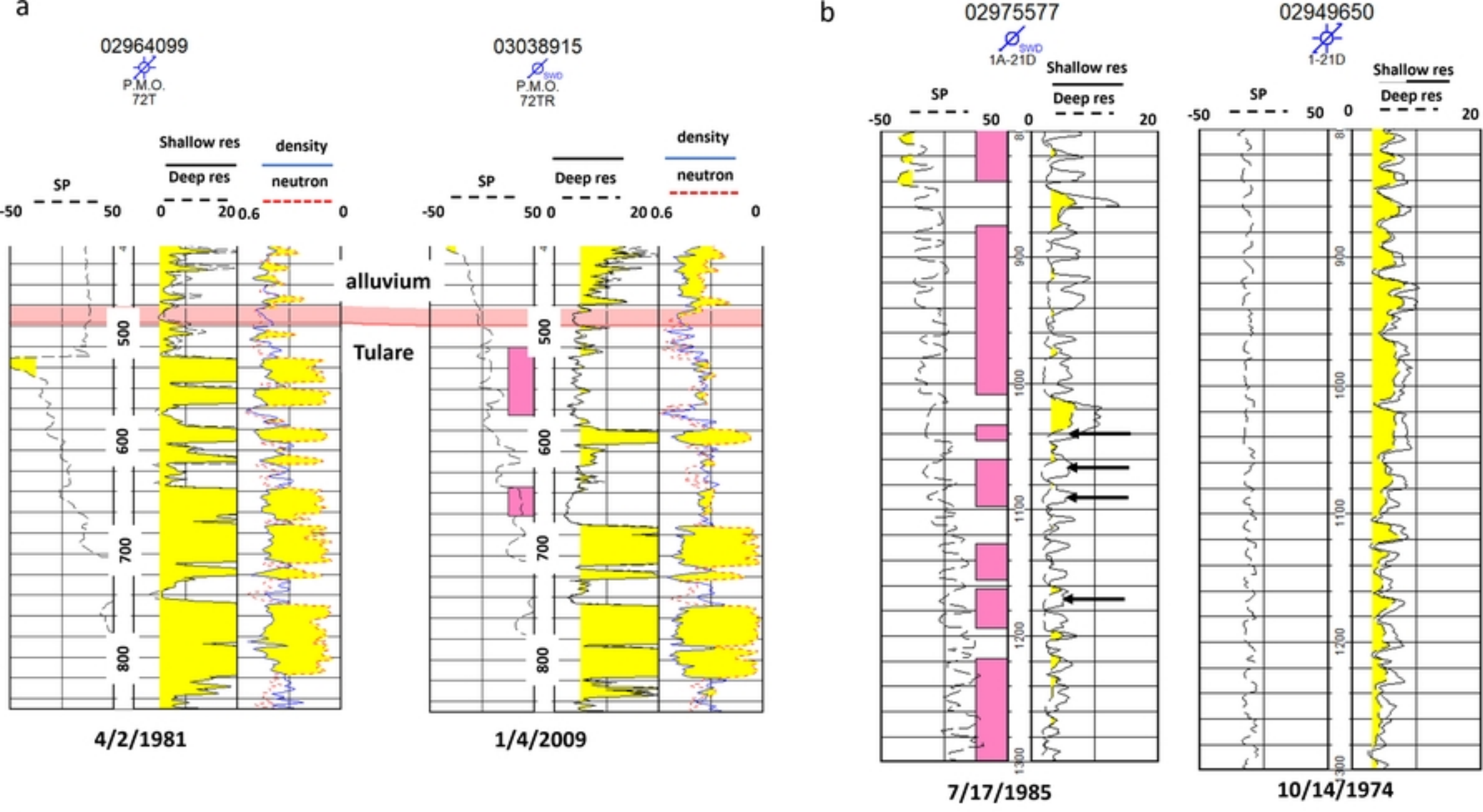
a
02964099
P.M.O.
72T
03038915
SWD
P.M.O.
72TR
Shallow res
Deep res
density
neutron
SP
-50
50
0
20
0.6
0
alluvium
Tulare
500
600
700
800
4/2/1981
1/4/2009
b
02975577
SWD
1A-21D
02949650
1-21D
900
1000
1100
1200
1300
7/17/1985
10/14/1974

Figure

a

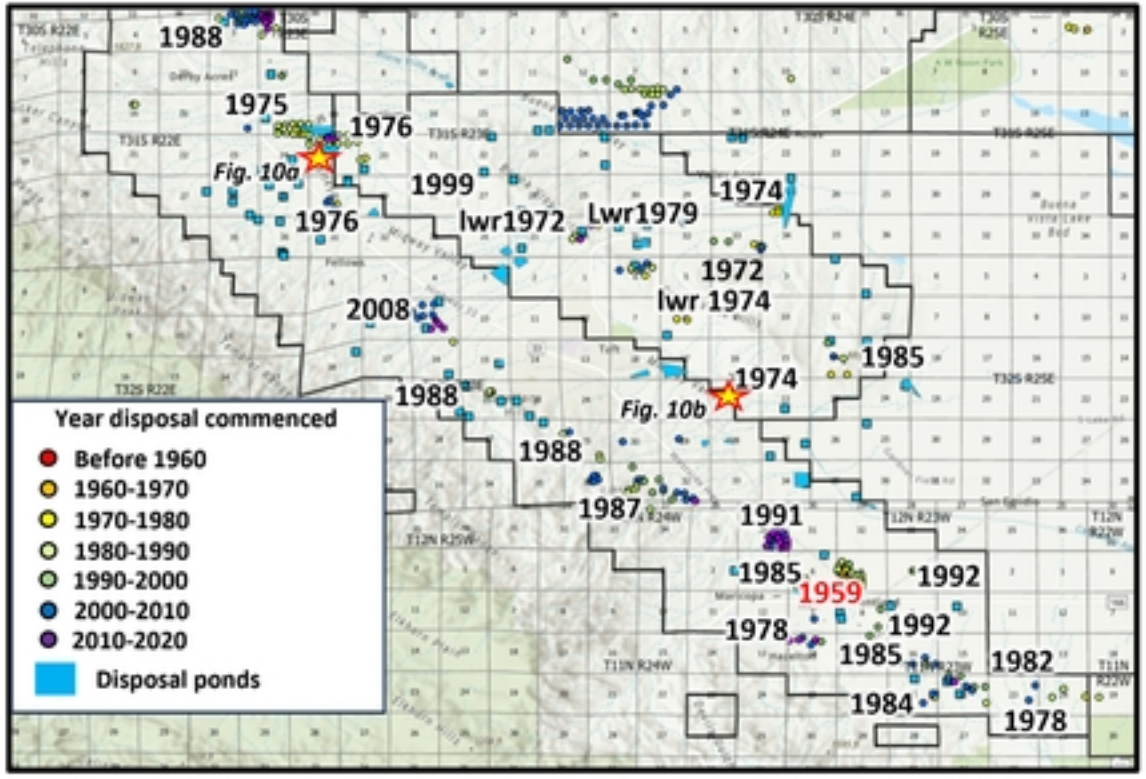
1988
1975
1976
Fig. 10a
1999
1976
lwr1972
Lwr1979
1974
1972
lwr 1974
2008
1985
1974
Fig. 10b
1988
1988
1987
1991
1985
1959
1992
1978
1992
1985
1982
1984
1978
Year disposal commenced
Before 1960
1960-1970
1970-1980
1980-1990
1990-2000
2000-2010
2010-2020
Disposal ponds

b

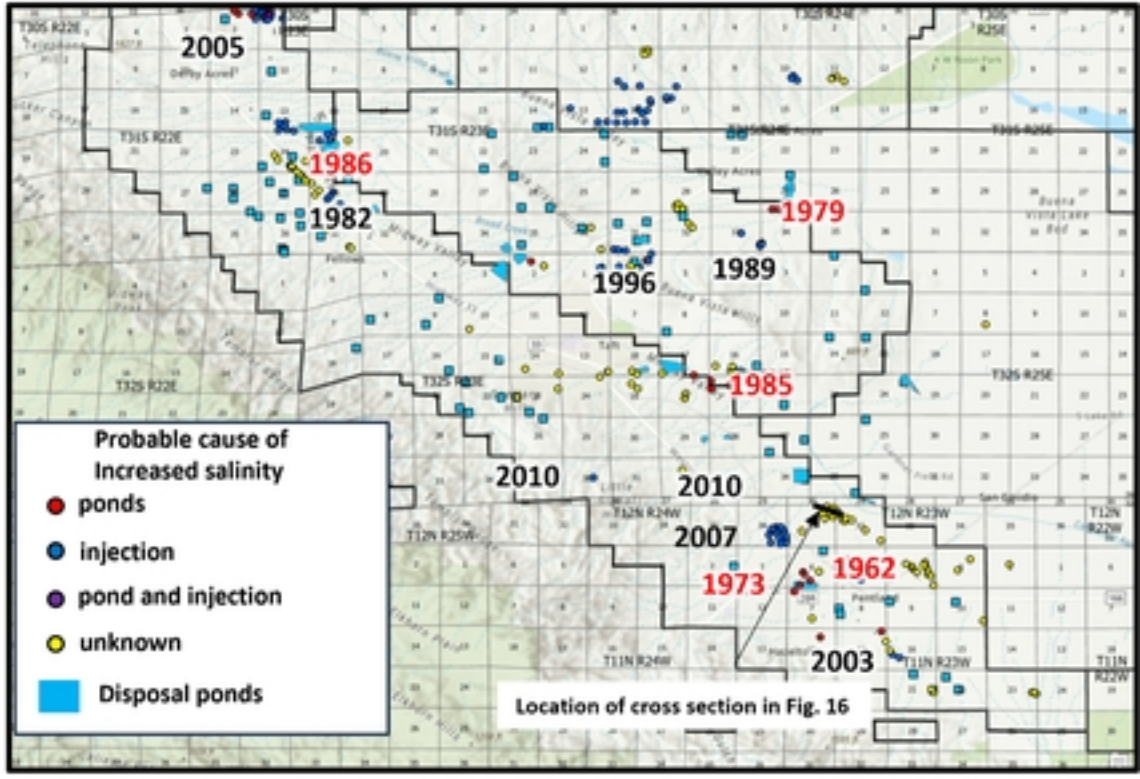
2005
1986
1982
1979
1989
1996
1985
2010
2010
2007
1973
1962
2003
Probable cause of Increased salinity
ponds
injection
pond and injection
unknown
Disposal ponds
Location of cross section in Fig. 16

Figure

a)


wells by completion year
500
450
400
350
300
250
200
150
100
50
0
1908-1920
1920-1930
1930-1940
1940-1950
1950-1960
1960-1970
1970-1980
1980-1990
1990-2000
2000-2010
2010-2020

b)

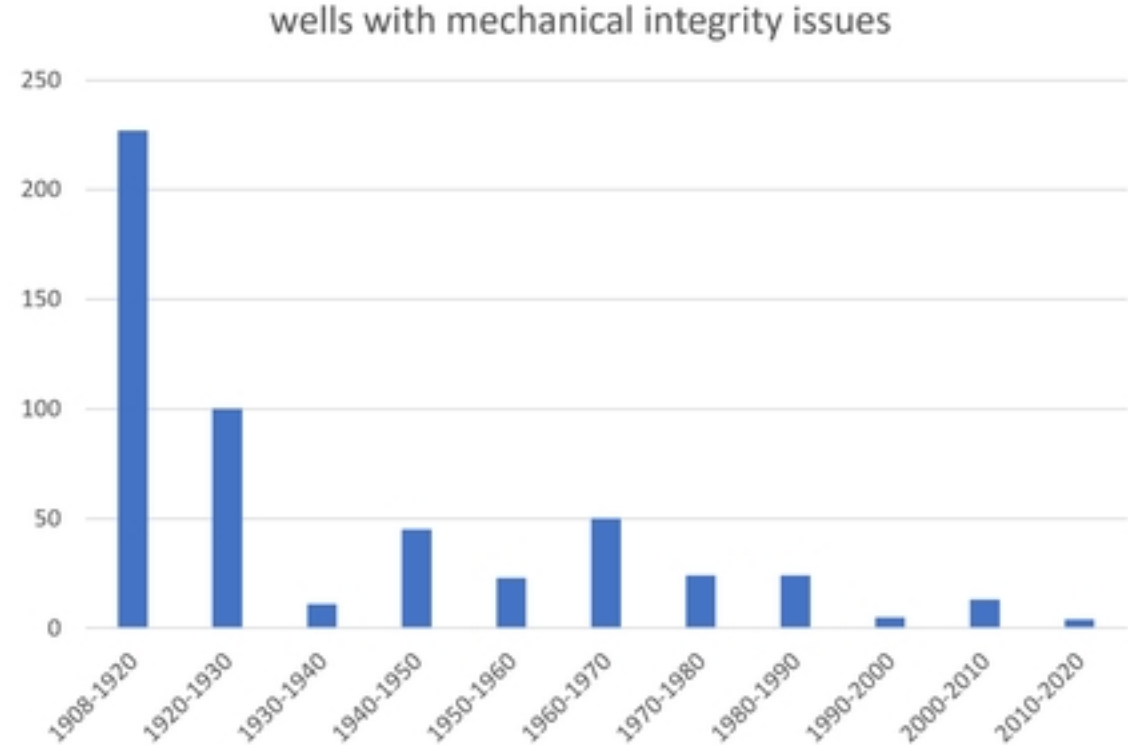
wells with mechanical integrity issues
250
200
150
100
50
0
1908-1920
1920-1930
1930-1940
1940-1950
1950-1960
1960-1970
1970-1980
1980-1990
1990-2000
2000-2010
2010-2020

Figure

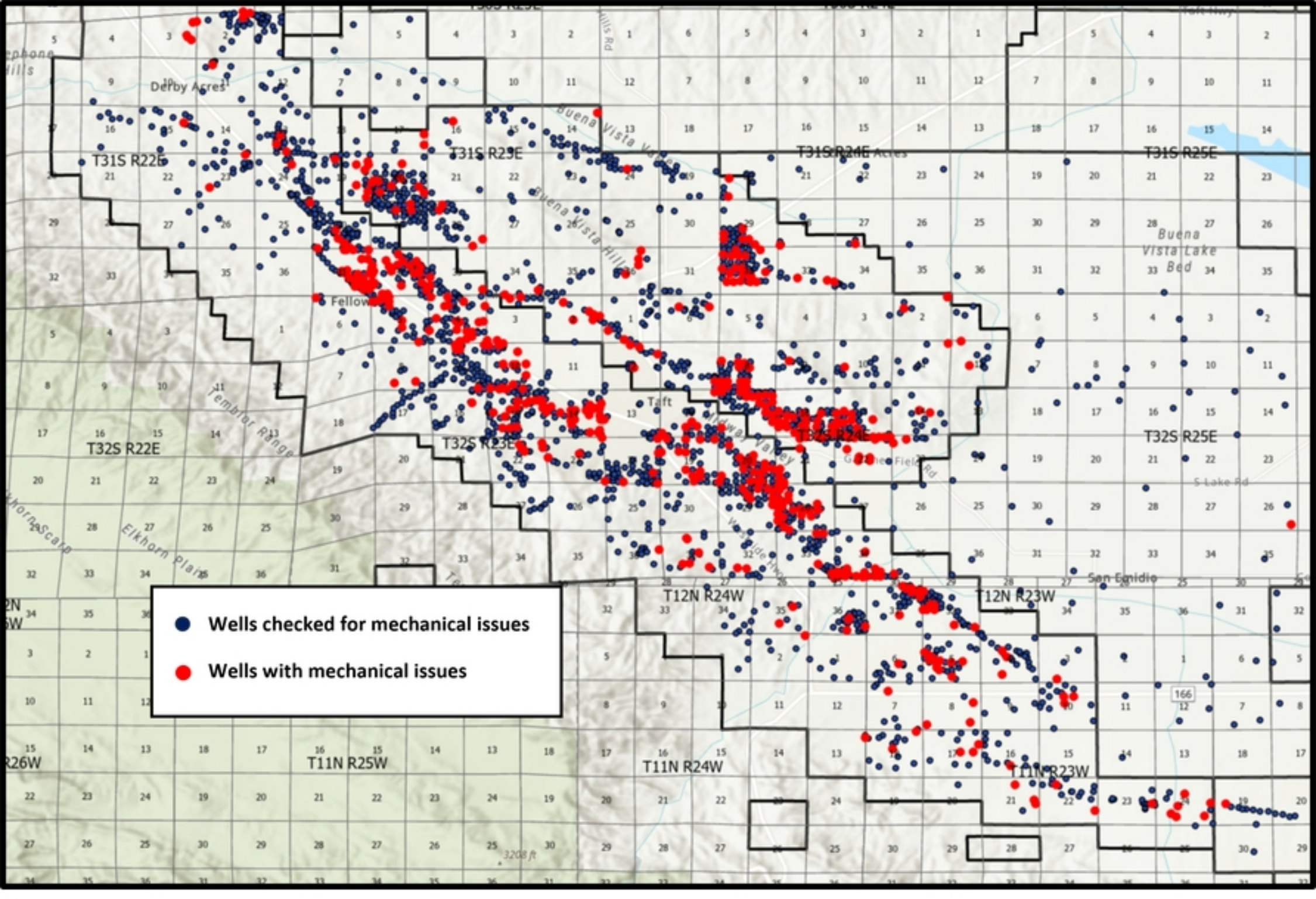
Wells checked for mechanical issues
Wells with mechanical issues
T31S R22E
T31S R23E
T31S R24E
T31S R25E
T32S R22E
T32S R23E
T32S R24E
T32S R25E
T12N R24W
T12N R23W
T11N R25W
T11N R24W
T11N R23W
Derby Acres
Buena Vista Hills
Buena Vista Lake Bed
Taft
Tembler Range
Elkhorn Plain
San Emidio

Figure

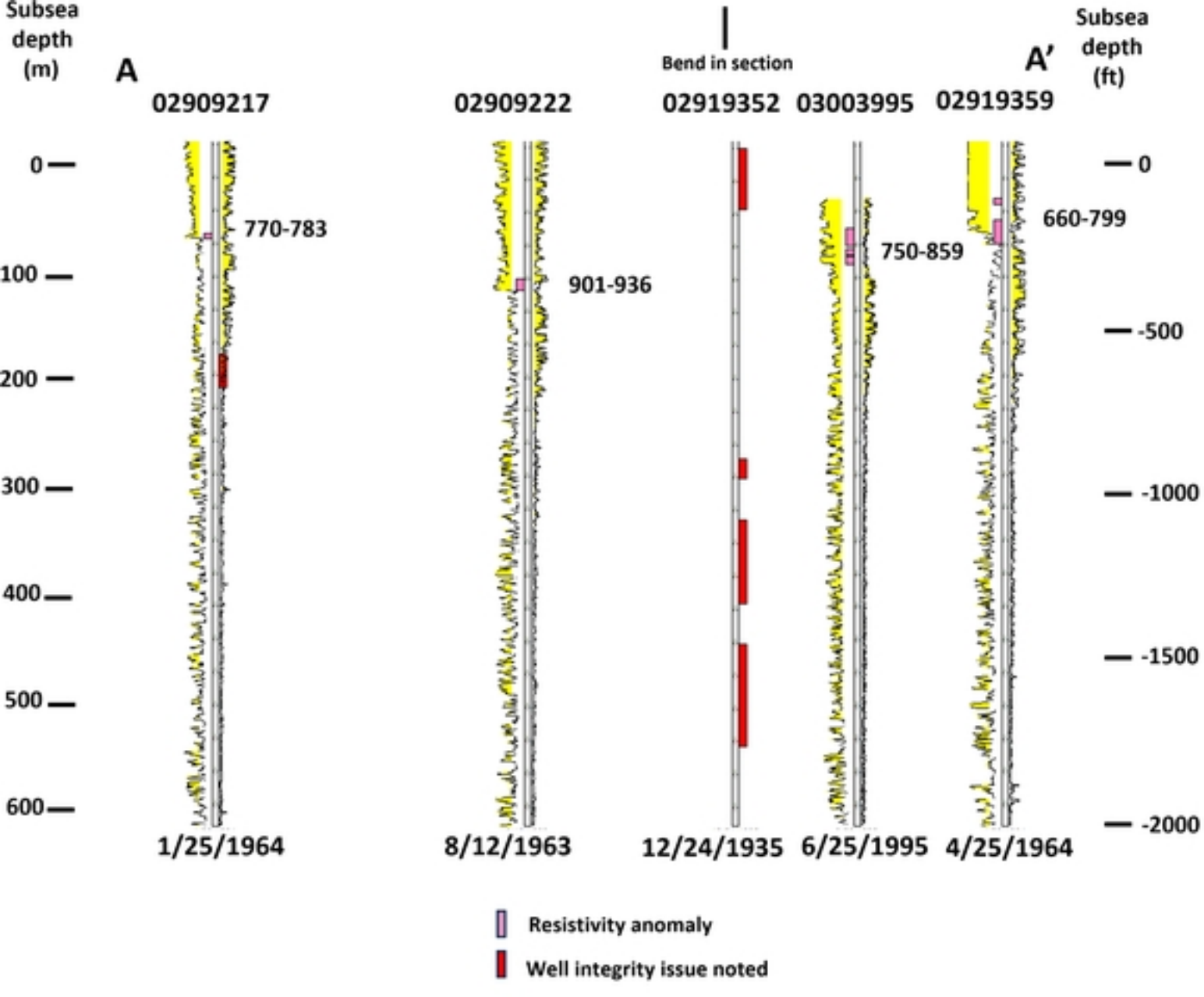
Subsea depth (m)
A
Bend in section
A'
Subsea depth (ft)
02909217
02909222
02919352
03003995
02919359
0
100
200
300
400
500
600
770-783
901-936
750-859
660-799
0
-500
-1000
-1500
-2000
1/25/1964
8/12/1963
12/24/1935
6/25/1995
4/25/1964
Resistivity anomaly
Well integrity issue noted

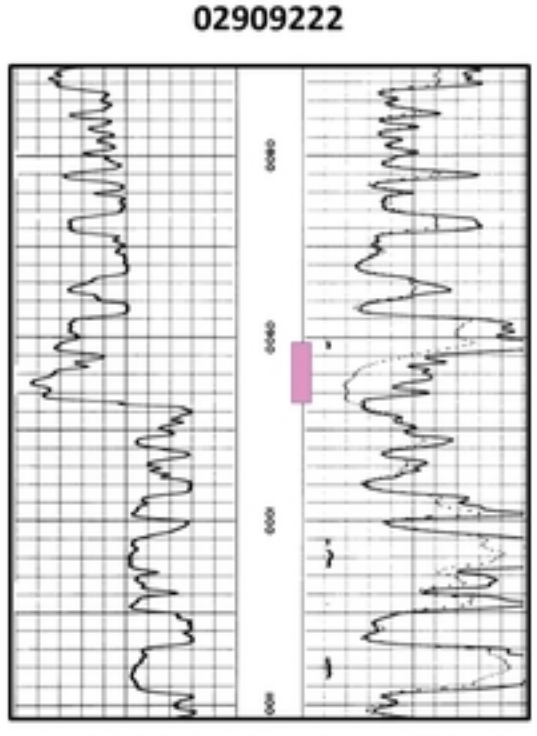
02909222

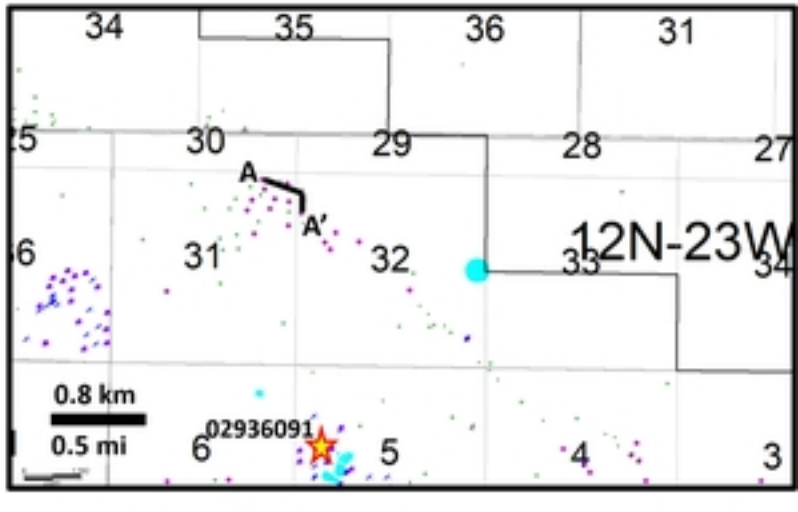
34
35
36
31
30
29
28
27
A
A'
31
32
33
12N-23W
0.8 km
0.5 mi
02936091
6
5
4
3

Figure